13

CRYSTALLIZATION DESIGN AND SCALE-UP

ROBERT RAHN MCKEOWN

Chemical Development, GlaxoSmithKline, Research Triangle Park, NC, USA

JAMES T. WERTMAN AND PHILIP C. DELL'ORCO

Chemical Development, GlaxoSmithKline, King of Prussia, PA, USA

13.1 INTRODUCTION

Crystallization can be defined as the formation of a solid crystalline phase of a chemical compound from a solution in which the compound is dissolved. In the synthesis of fine chemicals and pharmaceuticals, crystallization is extensively employed to achieve separation, purification, and product performance requirements. Despite its industrial relevance, an understanding of crystallization as a unit operation is often de-emphasized in engineering curricula and "learned on the job" in industrial settings.

In order to improve the knowledge and practice of crystallization science, several excellent volumes have been published that provide a comprehensive treatment of the subject [1–3]. The objective of this chapter is not to repeat these comprehensive overviews, but rather to provide a concise, basic understanding of crystallization design and scale-up principles, which can be applied toward common industrial problems. The focus is primarily on batch rather than continuous crystallization processes, as batch crystallization is the predominant processing method used in the pharmaceutical industry today.

The chapter begins with a discussion of crystallization design objectives and constraints on design, including a description of physical properties important to product performance. Thermodynamic principles of crystallization are then reviewed, followed by a discussion of crystallization kinetics. Crystallization design approaches are then presented, incorporating thermodynamic and kinetic considera-

tions. Finally, the scale-up and scale-down of heat and mass transfer are discussed. Throughout the chapter, industrially relevant examples are used to illustrate the concepts presented.

13.2 CRYSTALLIZATION DESIGN OBJECTIVES AND CONSTRAINTS

Crystallization is used in pharmaceutical synthesis to accomplish the following two objectives: (1) separation and purification of organic compounds and (2) delivery of physical properties suitable for downstream processing and formulation. In achieving these objectives, a crystallization design is constrained by economic and manufacturing considerations, such as yield, throughput, environmental impact, and the ability to scale the process. An overview of these topics is presented in this section.

13.2.1 Separation and Purification

The synthesis of an active pharmaceutical ingredient (API) from raw materials involves a multistep synthetic procedure during which the raw materials undergo numerous chemical transformations and purification steps to ultimately prepare the desired molecular structure in high purity, (typically >99%). One of the first steps in overall process design is to understand where isolated intermediates are required to meet purification needs. An example from the literature
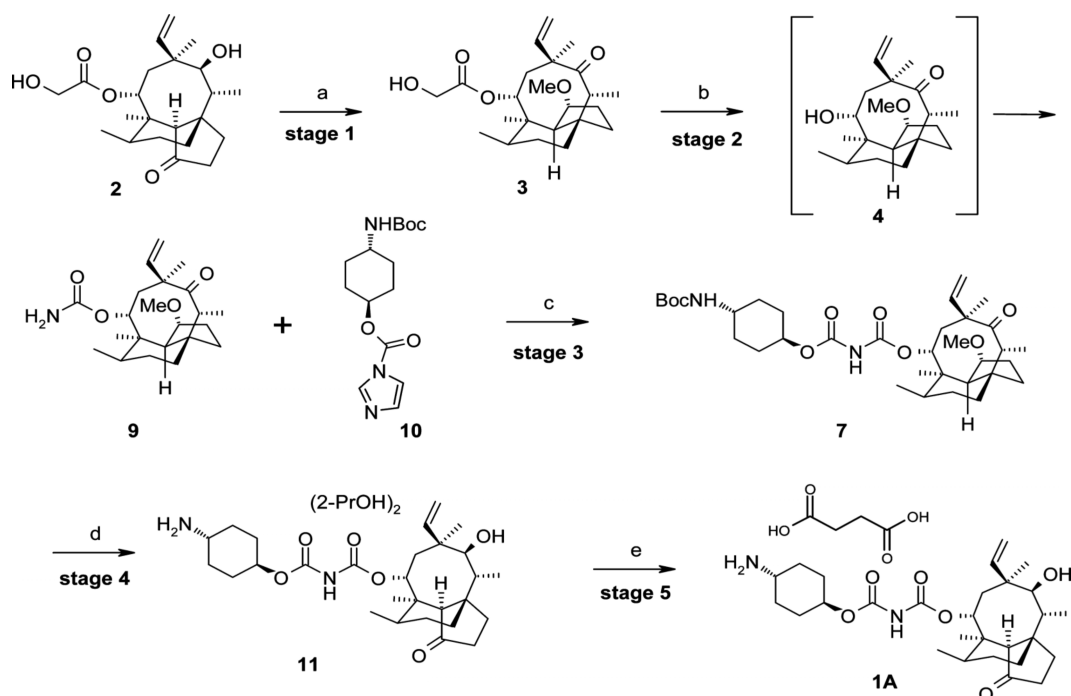
FIGURE 13.1 Schematic of a typical synthetic route to an active pharmaceutical ingredient [4]. This particular route uses six chemical transformations with five crystallizations to achieve the purity required to ensure product quality. Reprinted with permission from Ref. 4. Copyright (2009) American Chemical Society.

is used to exemplify a synthetic route and its separation/purification challenges. This example is illustrated in Figure 13.1 [4].

For the example in Figure 13.1, the API is produced in five stages from raw materials. Four of these five stages have crystallization steps to achieve purification, while the final stage uses a crystallization to control the composition and physical properties of the final molecule. The reference describes in detail the rationale for the placement of crystallization steps. Briefly, the stage 1 process was used to control key impurities in the process, as the input raw material 2 had approximately 35 impurities with the reaction producing additional impurities. This stage used a design space approach across the reaction and crystallization to ensure complete purging of raw material 2 at levels up to 3% and of an alkene impurity on the cyclohexyl ring of intermediate 3 at levels up to 4%. Crystallizations in stages 2, 3, and 4 increased the organic purity of the product from approximately 97% to greater than 99% prior to stage 5 so that this step could focus solely on the formation of the desired salt and control of resultant physical properties. Moreover, the use of crystallization in this synthesis allows intermediates to be "stabilized" by forming a less reactive solid phase, preventing solution phase side reactions (e.g., racemization), and allowing for material storage.

While organic impurities related to the molecular structure of the intermediates and products are one concern for product purification, inorganic and organic reagents also require separation. These include simple salts (e.g., NaCl, K_2CO_3, and NaOAc) and reagents (e.g., triethylamine, $Pd(OAc)_2$, and triphenylphosphine) commonly used in pharmaceutical synthesis. Crystallization is also used to control chiral purity, often through the use of chiral resolving agents [3].

Purification is enabled by selecting a solvent in which impurities are dissolved at the point where the desired product can be crystallized, or in which impurities remain undissolved and can be physically removed by filtration of the product solution. While thermodynamics are often the primary factor in achieving purification, kinetics may also impact the impurity content of a product by entrapment of impurities or solvents in the crystal lattice, often induced by rapid crystallization processes. This is discussed in additional detail in 13.5.3.

13.2.2   Product Performance

The second objective of crystallization is related primarily to API rather than to intermediate production. It concerns the delivery of the appropriate material physical properties to ensure acceptable downstream processing (e.g., isolation, drying, size reduction, and formulation unit operations) as well as the *in vivo/in vitro* performance of the formulated product. Of particular concern are the crystalline form of the compound, the particle size distribution of the active
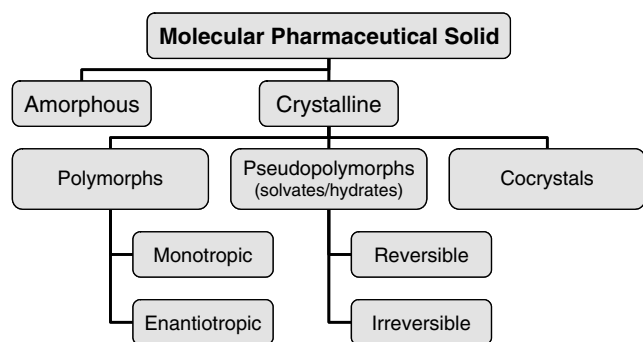
FIGURE 13.2 A map of the forms that a molecular pharmaceutical solid can exhibit. Crystalline materials are polymorphs, solvates/hydrates, and cocrystals. Cocrystals can be considered special cases of solvates, in which the "solvent" is instead an involatile compound that noncovalently bonds to the molecular solid in a regular, ordered manner. Irreversible solvates can convert either to polymorphs, different solvates, or amorphous materials upon desolvation/dehydration.

ingredient, and the morphology and flow properties of the product.

13.2.2.1 Crystalline Form Pharmaceutical solids are known for their ability to have multiple solid phases. A brief schematic of common solid phases is shown in Figure 13.2. Solid phases commonly exist as either "polymorphs" or "pseudopolymorphs." Pseudopolymorphs are also referred to as solvates and hydrates. Polymorphism occurs when a single compound exists in two or more solid-state forms that have identical chemical structures but different crystal lattice structures.

Polymorphs can have either "monotropic" or "enantiotropic" relationships [5]. This behavior is exhibited in Figure 13.3. When two polymorphs have a monotropic relationship they exhibit the same relative stability order up to the normal melting point of each polymorph. When an enantiotropic relationship exists, the polymorphs change stability order at a transition temperature below the normal melting point of either polymorph. In Figure 13.3, the Gibbs' free energy of two polymorphs is shown for both a monotropic case and an enantiotropic case. For the monotropic case (b), the Gibbs' free energy of polymorph I, G_I, is lowest across the temperature range until the melting point, where the liquid form of the material becomes most stable. In the enantiotropic case, polymorph II exhibits the lowest Gibbs' free energy, G_{II}, up to a transition temperature, IP_M at which point polymorph I exhibits the lowest Gibbs' free energy. As illustrated in Figure 13.3, the difference in enthalpy between polymorphs I and II (H_I and H_{II}) is approximately constant over the temperature range shown. Therefore, the change in their Gibbs' free energy relationship is predominately due to the entropy contribution, $T \Delta S$.
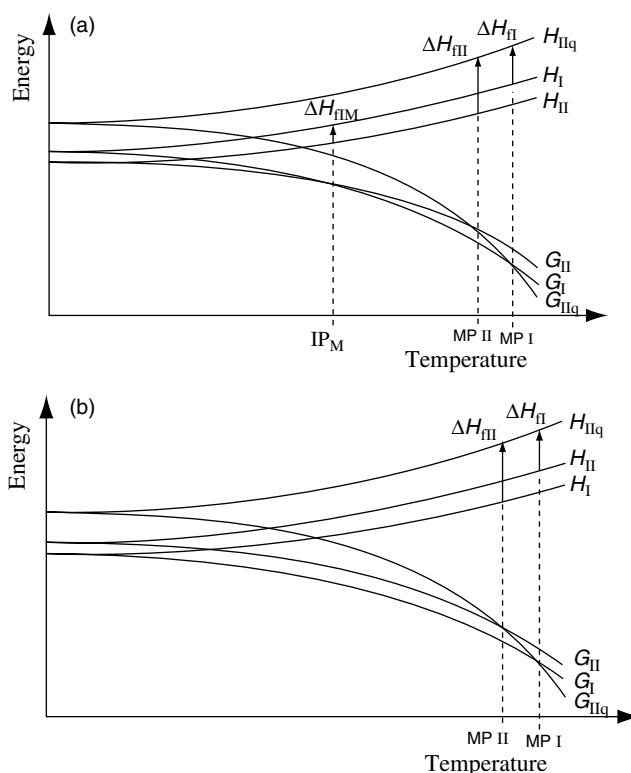
FIGURE 13.3 Thermodynamic description of polymorphism: enantiotropic (a) and monotropic (b) systems [6]. In the monotropic system, the stability order of forms is the same up to the melting point. For the enantiotropic system, a crossover temperature exists where the stability order changes. Reprinted with permission from Ref. 7. Copyright (1999) John Wiley & Sons, Inc.

Solvates and hydrates occur when a solvent or water molecule is integrated into the crystal lattice through a repeating, noncovalent bonding arrangement with the parent molecule. In the case of "reversible" solvates and hydrates, the molecule(s) of solvent or water can be removed from the pseudopolymorph without significantly affecting the crystallinity of the solid [8]. For "irreversible" pseudopolymorphs, removal of the solvent or water can lead to amorphous material. Amorphous material may also be produced through rapid precipitation or material comminution. Cocrystals are similar to solvates, except that the "solvent" or "water" molecule is instead an involatile solute (e.g., nicotinamide [9] and benzoic acid [10]), which forms a complex with the parent API via a repeating, noncovalent bonding pattern (typically through hydrogen bonding, π stacking, or van der Waals interactions between the parent and the solute). For a more in-depth discussion on crystalline forms, excellent texts are available [11, 12].

Crystalline forms are important because they may exhibit different properties, some of which can include

- Solubility
- Melting point

- Dissolution rate and bioavailability of a formulated solid dosage form
- Chemical and physical stability
- Habit and associated powder properties (e.g., flow, bulk density, and compressibility)

As a result, the desired crystalline form is typically defined prior to initiating a crystallization design. For an intermediate, the form is often selected based on ease of manufacture, filterability, and chemical and physical stability. For a final product, it is often chosen based on performance in the formulated product (e.g., bioavailability, dissolution rate, and chemical and physical stability) and on manufacturability (e.g., bulk density and melting point) [6, 13].

When designing a crystallization, it is frequently desired to produce the crystalline form that is most stable at the solution composition and temperature of isolation. If the form being produced is not thermodynamically stable, it is possible for form conversion to occur at some point in the life cycle of the product, with the unstable form becoming difficult or nearly impossible to manufacture. An excellent example of this is the oft-referenced Ritonavir example where a more stable form appeared during commercial manufacture and caused a disruption to supply while the form issue was resolved [14]. Because the conversion from an unstable to a stable form is a kinetic process, it can be affected by changes in impurities, equipment, concentration, and other process variables.

13.2.2.2 Particle Size
The second product performance criteria of concern is often particle size, although other properties such as surface area may be of equal or greater importance. The focus on particle size, and its frequent specification for APIs, is due to its potential impact on the performance of solid dosage forms:

1. Particle size can affect exposure to patients and *in vitro* specifications such as product dissolution. Product dissolution is a test where a formulated dosage form (e.g., tablet, capsule) is stirred in an aqueous media with the aqueous media measured for drug content as a function of time. The test is used to ensure consistency between drug product batches and is often correlated to exposure levels in patients. For example, crystals with larger particle sizes often dissolve more slowly than small particle size crystals, due to their lower surface area to volume ratio [15].

2. Particle size can affect final dosage form production by impacting powder conveyance and mixing. Conveyance and mixing can impact granulation (the drug product unit operation through which API is mixed with excipients, lubricants, and disintegrants prior to preparing the final dosage form, e.g., tabletting or capsule filling). It can also affect the dose uniformity (i.e., the amount of drug in each dosage unit) and drug product appearance (e.g., color and shape).

For a detailed discussion of particle size and the nature of particle size distributions, thorough descriptions have been prepared [1]. Briefly, particle size distributions in pharmaceutical manufacture typically utilize volume- or mass-based distributions. Mass-based distributions indicate what percentage of product mass is distributed into size intervals. Volume-based distributions indicate what percentage of product volume is distributed into size intervals. Mass and volume distributions are related to each other by the crystal density. Figure 13.4 displays a typical volume-based distribution for a pharmaceutical, with references made to d_{90}, d_{50}, and d_{10}. These values represent the particle size below which more than 90%, 50%, and 10% of the total volume of the product lies, respectively. Specifications for APIs often
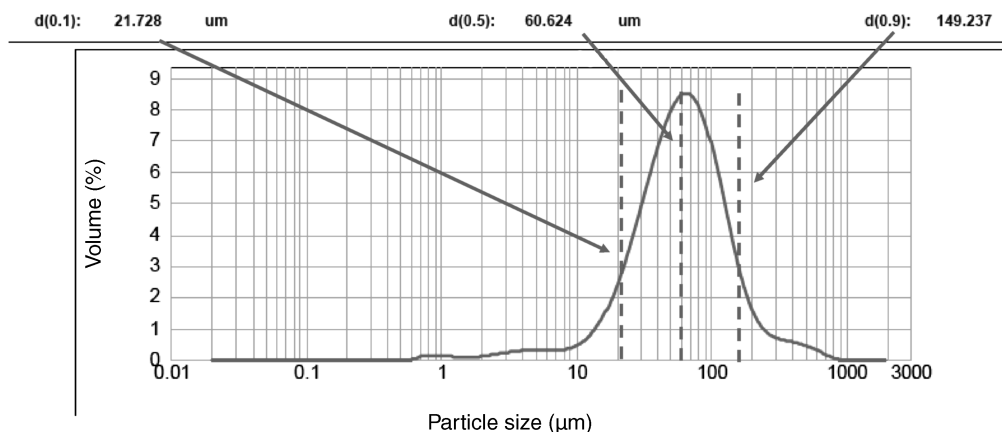
FIGURE 13.4 Particle size distribution (volume %) of a typical pharmaceutical product, measured by laser light diffraction. The $d(0.9)$ or d_{90} corresponds to the size at which 90% of the area of the curve is contained.

TABLE 13.1   Sieve Mass Fractions for an API

Sieve No.	Size Opening (μm)	Mass Retained on Sieve (g)	Sieve No.	Size Opening (μm)	Mass Retained on Sieve (g)
–	0	0.2	No. 30	595	12.2
No. 80	177	0.7	No. 25	707	8.7
No. 70	210	1.3	No. 20	841	5.3
No. 60	250	2.7	No. 18	1000	3.2
No. 50	297	5.3	No. 16	1190	2.4
No. 45	354	7.8	No. 14	1410	1.2
No. 40	420	10.9	No. 12	1680	0
No. 35	500	13.3	No. 10	2000	0

contain a range for particle size that includes one or more of d_{90}, d_{50}, and d_{10}. While the example in Figure 13.4 reflects a measurement obtained through a laser light scattering method for particle sizing, alternative methods such as sieving (which generates a mass distribution) are still routinely employed. Example 13.1 illustrates a mass particle size distribution calculation using sieves.

EXAMPLE 13.1   PARTICLE SIZE DISTRIBUTION CALCULATIONS

Seventy-five grams of API have been sieved using a cascade of 15 sieves. The mass on top of each sieve has been weighed, and is shown in Table 13.1. For mass distributions, instead of d_{90}, d_{50}, and d_{10}, the terms x_{90}, x_{50}, and x_{10} are used, where x represents mass fraction. Estimate the x_{90}, x_{50}, and x_{10} for the material.

For sieving, the first step is to assign a particle size to each interval. The amount on top of a sieve has a particle size that

is between the size opening of that sieve and the next largest sieve size opening. The particle size of this interval is estimated by averaging these two sieve size openings. Once this is done for all size intervals, the mass amount is tabulated as a function of particle size. The mass amounts are then cumulatively added across sieve sizes with the amount at each interval divided by the total amount of material input to the sieve test. This gives a cumulative percentage of mass retained as a function of particle size. The mass retained and the cumulative percentage mass are then plotted as a function of particle size (Figure 13.5). The x_{90} can be estimated as the particle size at which the cumulative mass is 90%. A similar approach is used for x_{50} and x_{10}, giving values of $x_{90} = 890$ μm, $x_{50} = 520\,\mu$m, and $x_{10} = 300\,\mu$m.

13.2.2.3   Morphology and Powder Flow Properties
A knowledge of crystal habits is important in understanding the particle size distribution and the behavior of powders and slurries, as different crystalline habits have different characteristic lengths and different flow characteristics. Flow
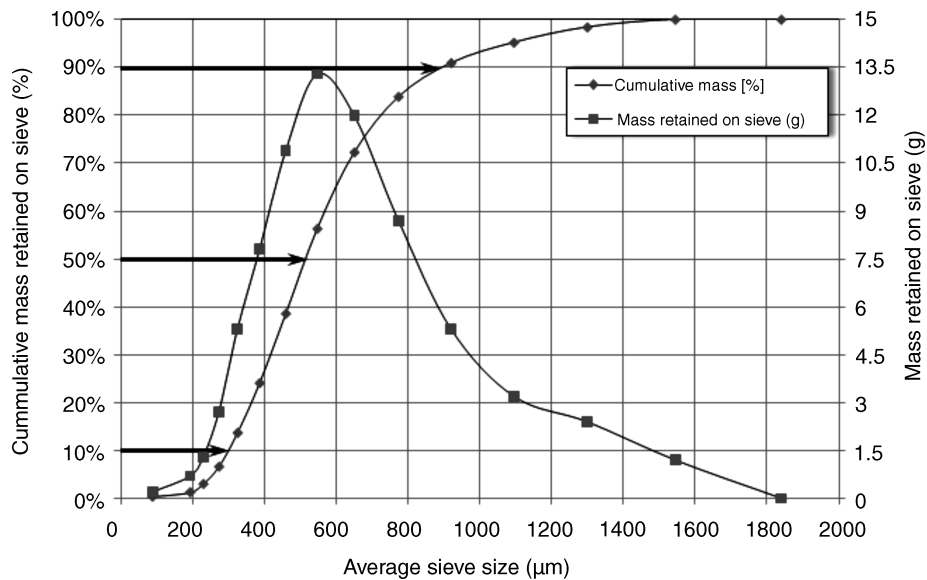
FIGURE 13.5   Size distribution estimated from sieve analysis data. Details of plot are described in Example 13.1.

characteristics are important because poor flowing powders can influence the ability of a powder to blend with excipients and can also impact the flow of powder in primary and secondary unit operations, causing undesirable phenomena such as core flow, also known as "rat-holing," in powder feed hoppers. The desired state for powder flow in a hopper is known as mass flow. In mass flow, the entire hopper contents are in motion. Mass flow is indicated by "first in–first out" flow of material, and a solid surface that sinks evenly. Core flow, on the contrary, is characterized by dormant zones near the walls of the hopper. Core flow is exemplified by a "last in–first out" flow of material and a solid surface that forms a core or rat-hole down the center of the hopper.

Figure 13.6 displays a summary of common habits observed in pharmaceutical crystallizations. Equant/block and bipyramidyl habits typically result in products that are easy to isolate, dry, and handle due to their relatively low surface area to volume ratio. Acicular and thin blade crystals, which are common in pharmaceuticals, tend to pose more processing difficulties such as long isolation times, agglomeration, and poor flow and handling properties. Despite processing difficulties, these habits may also result in high surface area materials, which can positively impact *in vivo* performance of a formulation. One of the key determinants of habit is the selected salt or hydration/solvation state of the parent molecule (i.e., the "version" of the molecule). The version and the selected form of that version, often selected early in development, can dictate the habit and constrain the ability to optimize downstream processing steps. The habit of a crystal may also be influenced by the crystallization solvent and the impurities present in the crystallization process.

The flow characteristics of a powder are frequently inferred from knowledge of powder densities, commonly the bulk and tapped densities. The bulk density of a powder is the density measured "as is," while the tapped density uses mechanical "taps" to facilitate further packing and settling of the powder. The ratio of the tapped to bulk density is referred to as the Hausner ratio, and provides an indication of the compressibility of powders and as a result the ease of powder conveyance. Materials with a Hausner ratio of less than 1.2 are generally considered to have acceptable flow properties, while those with a ratio greater than 1.4 are considered to have poor flow properties. The absolute values of density are also important, as they affect the level of fill for a piece of equipment. If material A has twice the bulk density of material B, the size of a batch can potentially be twice as large in the same equipment, resulting in increased throughput. Acicular materials routinely have Hausner ratios >1.3 and bulk densities <0.2 g/cm^3, while block and equant habits often have bulk densities >0.3 g/cm^3 and Hausner ratios <1.2 [16]. In addition to habit, particle size also affects material bulk densities, often proportionately (i.e., larger particle size generally corresponds to higher densities).

13.2.2.4 Manufacturability

Common manufacturability criteria include yield, cycle and batch times, environmental impact, and processability. Theoretical process yields are calculated with equilibrium solubility data, as described in the next section. Environmental impacts are often dictated by the toxicity of the solvent (ICH Class 3 solvents being preferred), amount of solvent used (<10 L/kg solute preferred), ability to recover the solvent (single solvent systems preferred), and boiling point of the solvent (55–100°C preferred). Cycle and batch times are affected by the time it takes for the crystallization to proceed, and by the time spent in the isolation and drying unit operations. Generally, smaller

| Acicular | Blade | Columnar |
| Plate | Block (or Equant) | Bipyramidal (also Equant) |
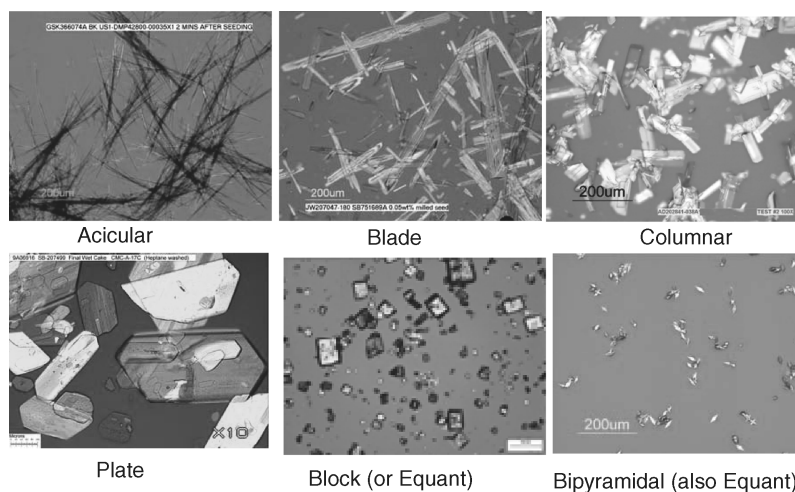
FIGURE 13.6 Commonly observed habits in pharmaceutical crystallization. For a more complete description of habits, please see Ref. 1.

particles will result in a higher filter cake resistance due to more efficient packing and reduced cake porosity [17]. As a result there is often a trade-off between time spent in each unit operation, as rapid crystallizations generate small particles (resulting in a slow isolation) and slow crystallizations generate larger particles (resulting in a rapid isolation). The integration of crystallization, isolation, and drying must be considered to deliver an optimum throughput for a product. An example of batch time analysis for a crystallization and isolation process is shown in Example 13.2.

EXAMPLE 13.2 ESTIMATION OF OPTIMAL CYCLE TIME FOR A CRYSTALLIZATION, ISOLATION, AND DRYING PROCESS

The API shown in Figure 13.7 is prepared by reactive crystallization where a base, ethylene diamine, is added to a molecular free acid. Two potential crystallization processes have been identified that meet the product performance needs.

Process 1 is performed in *tert*-butyl methyl ether (TBME), and requires 12 h to crystallize. Process 2 is performed in isopropyl alcohol (IPA), and requires 5 h to crystallize. Both crystallizations use 10 L solvent/kg product, the yields for both processes are the same, and both processes are isolated at 20°C. Either process is planned to use a 1 m^2 area filter with a mass loading of 100 kg and a 1 barg filtration pressure. Filter cake resistances, α, of the products were measured through small-scale tests to be 1.0×10^{11} and 0.5×10^{11} m/kg, respectively, where the cake resistance is estimated through equation 13.1, assuming a negligible media resistance. In equation 13.1, t is the filtration time, m_f is the mass of filtrate, ν is the kinematic viscosity, c is the mass of solids per mass of filtrate, A_F is the filtration area, and P is the pressure drop across the filter.

$$\frac{t}{m_f} = \frac{\alpha \nu c}{2A_F^2 P} m_f \qquad (13.1)$$

Which process offers the minimum batch time, and by how much (assume 1 bar atmospheric pressure)?
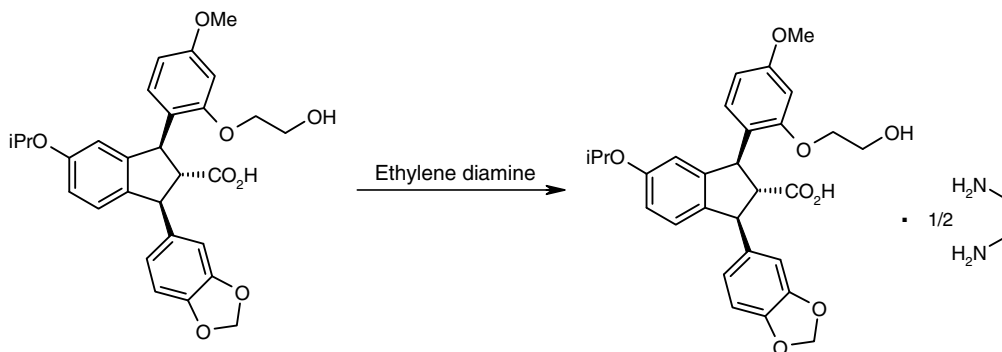
Solution

The filtration time for each material must be estimated at commercial scale. At 20°C, TBME has a kinematic viscosity of 4.7×10^{-7} m^2/s and a density of 0.740 kg/L, while IPA has a kinematic viscosity of 2.9×10^{-6} m^2/s and a density of 0.786 kg/L. From the equation provided, the isolation times for a 100 kg batch with 10 L solvent/kg product can be estimated as

$$c = \frac{1\,kg}{10\,L} \cdot \frac{1\,L}{0.740\,kg} = 0.135 \quad \text{and}$$

$$m_f = 10\,L/kg \cdot 100\,kg \cdot 0.740\,kg/L = 740\,kg$$

$$t = \frac{\alpha \nu c}{2A_F^2 P} m_f^2$$

$$= \frac{1.0 \times 10^{11}\,m/kg \cdot 4.7 \times 10^{-7}\,m^2/s \cdot 0.135}{2 \cdot (1\,m^2)^2 \cdot (1 \times 10^5\,kg/m\,s^2)} \cdot (740\,kg)^2$$

$$= 17390\,s \Rightarrow t = 4.8\,hr \text{ for the TMBE process filtration}$$

$$c = \frac{1\,kg}{10\,L} \cdot \frac{1\,L}{0.786\,kg} = 0.127 \text{ and}$$

$$m_f = 10\,L/kg \cdot 100\,kg \cdot 0.786\,kg/L = 786\,kg$$

$$t = \frac{\alpha \nu c}{2A_F^2 P} m_f^2$$

$$= \frac{0.5 \times 10^{11}\,m/kg \cdot 2.9 \times 10^{-6}\,m^2/s \cdot 0.127}{2 \cdot (1\,m^2)^2 \cdot (1 \times 10^5\,kg/m\,s^2)} \cdot (786\,kg)^2$$

$$= 56985\,s \Rightarrow t = 15.8\,h \text{ for the IPA process filtration}$$

So the total batch time using TBME is $12 + 4.8 = 16.8$ h and using IPA is $5 + 15.8 = 20.8$ h. TBME offers a lower batch time by 4 h, mainly due to the lower kinematic viscosity of TBME compared with IPA. More detailed approaches optimizing crystallization parameters in-line with isolation times can be performed [18].

Example 13.2 illustrates a key aspect of crystallization design that is also illustrated in Figure 13.8. The crystallization

FIGURE 13.7 Example reactive API crystallization process. Details are described in Example 13.2.
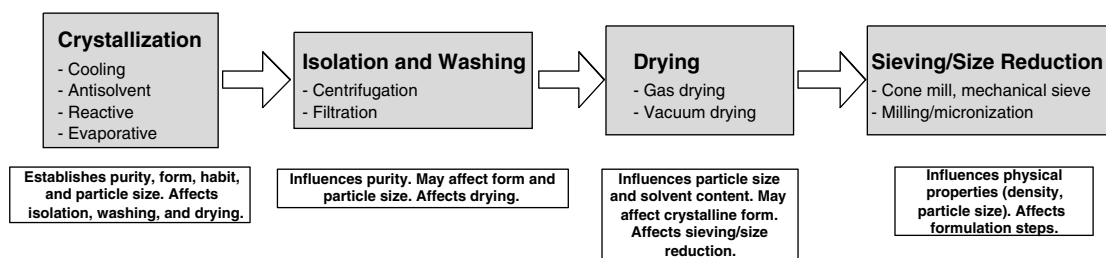
FIGURE 13.8   The relationships of crystallization with downstream processing steps. Crystallization typically needs to be studied in conjunction with downstream steps to understand the complete control of desired attributes.

in the example affects isolation performance, which in turn affects drying performance, which affects sieving and size reduction performance, which ultimately affects performance in the formulation process. As a result, it is often necessary to study crystallization in conjunction with several unit operations. As shown in Example 13.2, it is straightforward to assess the dependence of the crystallization on the isolation step and the drying step can further be integrated into structured studies. Each downstream unit operation must be investigated for its impact in ensuring the process, and not just the crystallization, achieves the desired performance objective.

13.3   SOLUBILITY ASSESSMENT AND PRELIMINARY SOLVENT SELECTION

An understanding of a compound's solubility is the starting point for crystallization design. The solubility of a compound determines the throughput and yield; it is the key measurement for selecting a solvent system and selecting a crystallization mode. Solubility is a thermodynamic property of a solute, which describes the equilibrium of a defined solid phase (e.g., a polymorph or pseudopolymorph) with a solution, as shown in equation 13.2. It is a dynamic equilibrium whereby the rate of dissolution is balanced by the rate of crystallization.

$$\text{drug(dissolved)} \xleftrightarrow[k_{\text{dissolutioin}}]{k_{\text{crystallize}}} \text{drug(s)} \qquad (13.2)$$
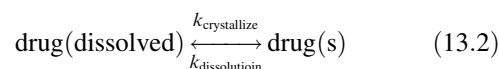
Solubility is determined through equilibrium experiments in which a solid phase is slurried isothermally with a solvent until a constant concentration is achieved in the solution phase. Typical solubility data collection for a pharmaceutical compound is shown in Figure 13.9. These data illustrate the general approach to measurement: solid of a known phase is
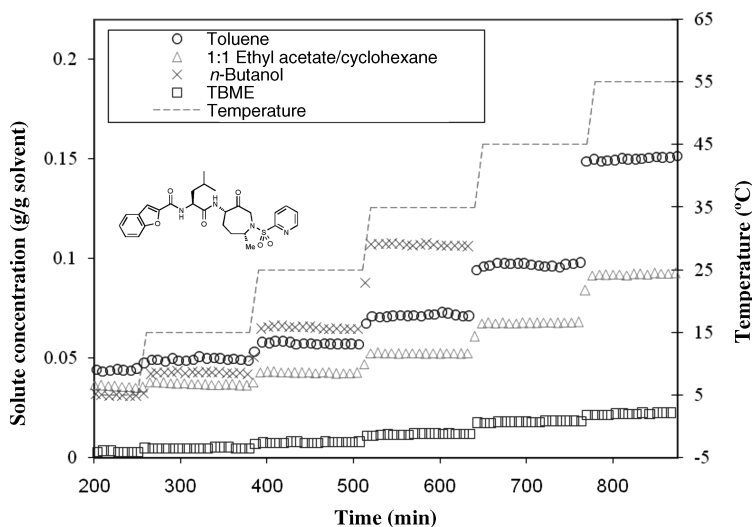
FIGURE 13.9   Results from a solubility experiment using Diamond Attenuated Total Reflectance IR spectroscopy to measure concentration *in situ* for a pharmaceutical active ingredient. At increasing temperatures, the solute achieves an equilibrium in the different solvent mixtures, indicated by the plateau in concentration upon achieving a new temperature. In this case, equilibrium is rapidly achieved.

added to a predefined amount of solvent at low temperature, an equilibrium concentration is achieved, and the temperature is then increased, while ensuring solids are still present. At the end of the experiment, the solid phase of the material is assessed to ensure the crystalline form has not changed, as different forms have different equilibrium concentrations. If binary or ternary solvents are being studied, the phase composition of the mixture should also be measured at the end of the experiment to ensure no changes. Each compound possesses its own timescale in which equilibrium is achieved, which typically ranges from minutes to hours, although days may be required in some circumstances. As illustrated in Figure 13.9, in-line methods of solute concentration measurement are useful in understanding time to equilibrium. When in-line methods are not practical, measurement of the filtered equilibrium solution by HPLC (or gravimetric analysis if the material is relatively free from impurities) is commonly used.

While Figure 13.9 displays solubility as a function of temperature, it may also be measured as a function of solvent composition. When temperature is used to generate solubility differences, the result is a "cooling" crystallization. When solvent composition is used, the result is often called an "antisolvent" crystallization. In all cases, the preferred units of solubility are mass solute per mass solvent. These units are convenient for many engineering calculations.

Once data are collected, they can be evaluated for use in process design. The thermodynamic description of two phases in equilibrium is

$$f_i^{\text{solid}} = f_i^{\text{solution}} \qquad (13.3)$$

where f_i^{solid} is the fugacity of component i in the solid phase and f_i^{solution} is the fugacity of component i in the liquid or solution phase.

From this, one can derive an expression for solubility of the general form:

$$x_{\text{ideal}} = \frac{1}{\gamma_{\text{solute}}} \exp\left[\frac{\Delta H_{\text{tp}}}{R}\left(\frac{1}{T_{\text{tp}}} - \frac{1}{T}\right) - \frac{\Delta C_P}{R}\left(\ln\frac{T_{\text{tp}}}{T} - \frac{T_{\text{tp}}}{T} + 1\right)\right.$$
$$\left. - \frac{\Delta V}{RT}(P - P_{\text{tp}})\right] \qquad (13.4)$$

where x_{ideal} is the ideal solubility of the solute (mol solute/mol solution), γ_{drug} is the activity of the drug in solution, ΔH_{tp} is the enthalpy change for a liquid–solid solute transformation at the triple point, ΔC_P is constant pressure heat capacity difference between the liquid and solid solute phases, ΔV is the volume change, T is the temperature, T_{tp} the triple point temperature, P is the pressure, P_{tp} is the triple point pressure, and R is the universal gas constant.

In almost all situations, pressure has a little to no effect on solubility; therefore, the pressure term can be eliminated. The change in heat capacity is often assumed to be negligible,

and the triple point is often replaced with the melting point of the solid to yield the approximation shown below:

$$x_{\text{ideal}} = \frac{1}{\gamma_{\text{solute}}} \exp\left[\frac{\Delta H_{\text{m}}}{R}\left(\frac{1}{T_{\text{m}}} - \frac{1}{T}\right)\right] \qquad (13.5)$$

for an ideal solution, this can be reduced to a van't Hoff type expression and linearized

$$\ln x_{\text{ideal}}\gamma_{\text{solute}} = \ln(S_{\text{solute}}) = \frac{\Delta H_{\text{m}}}{RT_{\text{m}}} - \frac{\Delta H_{\text{m}}}{RT} = \frac{A_{\text{S}}}{T} + B_{\text{S}} \qquad (13.6)$$

where S_{solute} is the observed solubility and A_{S} and B_{S} are constants obtained by regression. For ease of use in future calculations, the natural log of solubility is taken with solubility often having units of mass of solute per mass of solvent and temperature having units of Kelvin (Figure 13.10).

Almost all solutions containing a high fraction of API are nonideal; however this linearization technique (i.e., plotting $\ln(S_{\text{solute}})$ versus $1/T$) is a simple way to visualize and interpolate solubility from a few data points. For systems in which these plots are nonlinear, a correction can be added to equation 13.6 [1]:

$$\ln(S_{\text{solute}}) = \frac{A_{\text{S}}}{T} + B_{\text{S}} + C_{\text{S}}\ln(T) \qquad (13.7)$$

where C_{S} is an additional constant. In other cases, polynomial or exponential functions may be used to represent data, but these expressions tend to be less representative when extrapolated beyond the range of temperature studied in the solubility experiment. When solubility is correlated as a function of both composition (solvent 1 and solvent 2) and temperature, A_{S} and B_{S} can often be empirically estimated as linear or quadratic functions of solvent 2 volume fraction to provide an adequate data fit.

Once solubility is measured, it can be used for a number of purposes. First, it can be used to select the crystallization solvent based on the design criteria: typically yield, throughput, and environmental constraints. The potential process yield, Y, is often estimated by equation 13.8 below:

$$Y = \frac{S_{\text{solute 1}} m_{\text{solvent 1}} - S_{\text{solute 2}} m_{\text{solvent 2}}}{S_{\text{solute 1}} m_{\text{solvent 1}}} \qquad (13.8)$$

In equation 13.8, S_{solute1} and S_{solute2} are the solubility at the dissolution temperature and composition, and the solubility at isolation temperature and composition, respectively, and m_{solvent1} and m_{solvent2} are the mass of solvent at the dissolution temperature and composition, and the mass of solvent at isolation temperature and composition, respectively.

Another use of solubility data is the estimation of purification potential for a crystallization. To perform this assessment, the solubility of the impurity must also be known. Using equation 13.8, it is possible to calculate the mass of
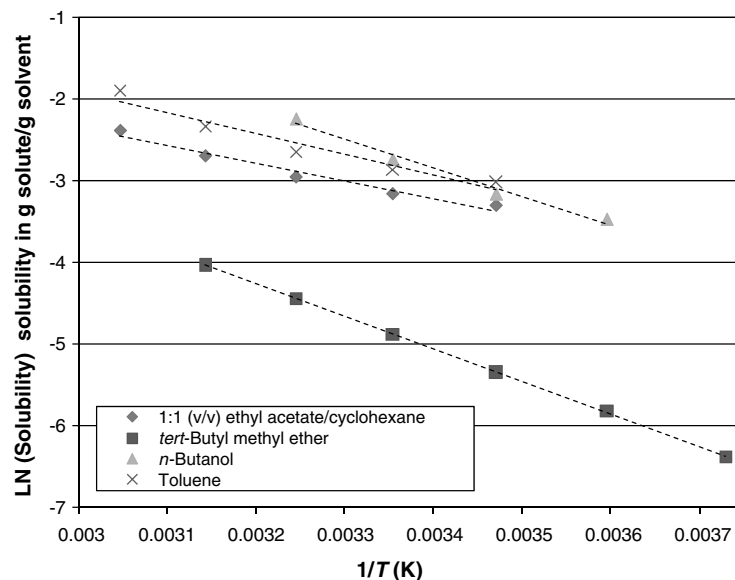
FIGURE 13.10   Solubility data from Figure 13.9 regressed using a simple van't Hoff relationship. For some solvents, the fit is very linear (e.g., *tert*-butyl methyl ether). Other solvents would benefit from an additional fitting parameter due to curvature (e.g., toluene) using the $C\ln(T)$ term, equation 13.7.

impurity and desired solute out of solution at the isolation temperature and composition, giving the potential product purity for the crystallization. The actual purification can be less than the calculated values due to impurity inclusion or occlusion in the product. The following example illustrates the use of solubility data to estimate the purification potential of a solvent.

EXAMPLE 13.3   USING SOLUBILITY TO PREDICT YIELD AND PURITY

(a) Given the solubility data in Table 13.2, calculate the maximum yield when the product is dissolved at 80°C and isolated at 10°C.

TABLE 13.2   API and Impurity Solubility Data for Example 13.3

Temperature (°C)	API Solubility (mg/mL solvent)	Impurity Solubility (mg/mL solvent)
0	1.8	0.9
10	3	1.2
20	6	1.7
30	10	2.2
40	15	2.7
50	22	3.3
60	33	4.1
70	50	5.0
80	78	6.2
90	120	7.7

(b) Given the additional data for the impurity, generate a graph of the yield and purity of the product versus dissolution temperature when isolating at 10°C with an input purity of 96%, assuming the impurity does not impact the API solubility.

Solution

(a) The yield can be calculated by performing a mass balance on the API in the solution phase. Equation 13.8 can be modified to equation 13.9, because the mass of solvent is the same at the beginning and end of the crystallization, and assuming the density of solvent does not change across the crystallization:

$$Y = \frac{S_{\text{solute 1}} - S_{\text{solute 2}}}{S_{\text{solute 1}}} \qquad (13.9)$$

Therefore, the yield for a saturated solution at 80°C isolated at 10°C can be calculated as:

$$Y_{\text{API}} = \frac{S_{\text{API}}(80°C) - S_{\text{API}}(10°C)}{S_{\text{API}}(80°C)} = \frac{78 - 3}{78} = 96.2\%$$

The yield of API for each dissolution temperature can be calculated using equation 13.9. However, the level of impurity will always start at 4% of the initial API concentration, not the solubility limit. Therefore, the yield of impurity can be calculated as (Figure 13.11):

$$\text{Purity} = \frac{m_{\text{API}}Y_{\text{API}}}{m_{\text{API}}Y_{\text{API}} + m_{\text{impurity}}Y_{\text{impurity}}}$$

$$= \frac{Y_{\text{API}}}{Y_{\text{API}} + (1 - \text{Purity}_{\text{input}})Y_{\text{impurity}}} \qquad (13.10)$$
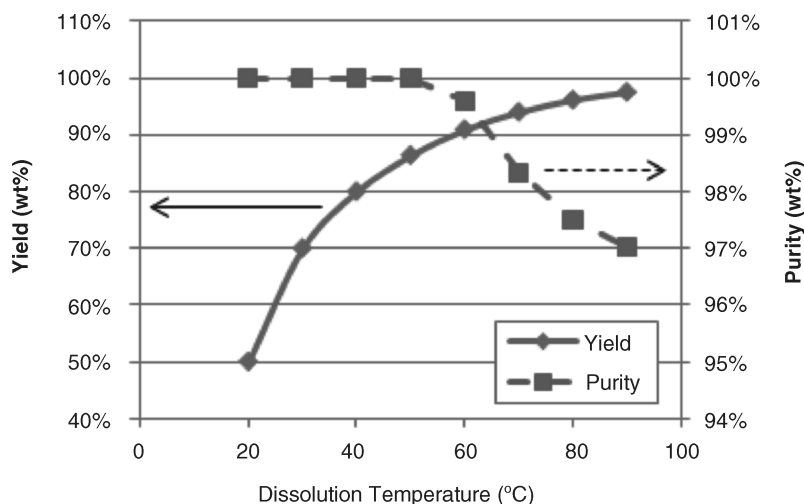
FIGURE 13.11 Illustration of the trade-off between API purity and yield varying the dissolution temperature (and solvent amount) with a constant isolation temperature. Details for the plot are described in Example 13.3.

An example of this calculation follows using the results from the first part, dissolution at 80°C and isolation at 10°C.

$$Y_{\text{impurity}} = \frac{0.04 \cdot S_{\text{API}}(80°C) - S_{\text{impurity}}(10°C)}{0.04 \cdot S_{\text{API}}(80°C)}$$

$$= \frac{0.04 \cdot 78 - 1.2}{0.04 \cdot 78} = 61.5\%$$

$$\text{Purity} = \frac{0.962}{0.962 + (1 - 0.96) \cdot 0.615} = 97.5\%$$

Solubility and related experiments are also essential in understanding the relative stability of crystalline forms. When slurrying solids at a constant composition and temperature, the crystalline form may stay the same or partially/fully convert to another form. If conversion occurs, the new form is more stable than the input form at that temperature and composition. The typical path for this type of process is shown in the scheme below for the formation of a hydrate from an anhydrate form:

$$A(s) + x\,H_2O(l) \Longleftrightarrow [A \cdot x\,H_2O](l) \Longleftrightarrow A \cdot x\,H_2O(s)$$
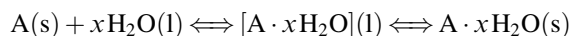
The anhydrate will initially dissolve, forming a dissolved and hydrated solute molecule. This hydrated species then spontaneously crystallizes as the more stable form, and the newly formed crystals continue to grow due to the higher solubility of the anhydrate relative to the hydrate. As the processes for spontaneous crystallization and growth can be slow, these experiments often take days or even weeks to achieve equilibrium. The process can be accelerated by performing the slurry experiment with both forms present

initially or through minor fluctuations in temperature (e.g., ±5°C).

The "simple" phase diagram that can be constructed to understand the critical solvent activity or concentration required to facilitate a form change is illustrated in Figure 13.12a [19]. Such studies would also be conducted as a function of temperature to give a full view of the phase diagram.

An example of the use of solubility to understand the relative stability of two anhydrous forms is shown in Figure 13.12b. In Figure 13.12b, the two forms exhibit an enantiotropic relationship and a "crossover" temperature where the forms change in stability order. The "crossover" temperature is easily estimated through extrapolation of solubility data.

The solubility of a compound can be dramatically affected by the presence of impurities or residual solvents. When measuring the solubility for crystallization design purposes, it is recommended that the first measurement be made on relatively "pure" materials (>98%) in pure solvents. This gives a baseline understanding of behavior in the absence of nonidealities. Then, measurements of representative materials in representative process solvents should be taken. The values in actual systems should be used for forward design purposes; the differences between "ideal" and actual systems can often be narrowed through an adjustment of the actual system (e.g., removal of an impurity or better control of small quantities of undesired solvent).

Nonidealities caused by compositional differences can often be used advantageously. A specific instance involves the use of water as a cosolvent for poorly soluble intermediates and APIs. Water, when present as a minor component of a solvent system, often has a dramatic solubility enhancement

(a)

(b)
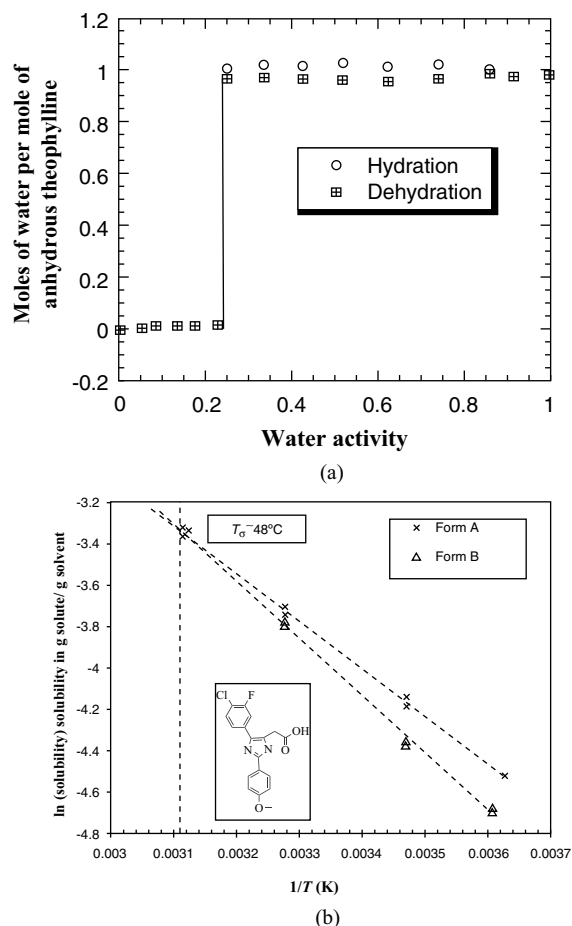
FIGURE 13.12 The use of equilibration and solubility experiments to understand form stability relationships. (a) Hydrate/anhydrate phase diagram that shows a critical water activity of ~0.25 needed to achieve full hydration. Below this activity, the anhydrate will be the most stable polymorph. The data was collected over 5 days starting from both 100% hydrate in one case (squares) and 100% anhydrate in the other case (circles) [19]. Reprinted with permission from Ref. 19. Copyright (1996) with permission from Elsevier.
(b) An enantiotropic system of an API. The solubility of Form B is less than the solubility of Form A at temperatures up to approximately 48°C (i.e., the crossover temperature), at which point Form A exhibits a lower solubility and becomes more stable.

effect that can be used advantageously, especially for compounds which exhibit poor solubility in neat solvents. This behavior is illustrated in Figure 13.13, in which a pharmaceutical compound exhibits a solubility maxima near 10% water content (158 mg API/g solvent), while exhibiting a low solubility in both neat solvent (28 mg API/g solvent) and pure water (0.1 mg API/g solvent).

Solvent evaluation using solubility data is essential to achieving many of the objectives for a crystallization: yield, throughput, and environmental impact (e.g., hazard of solvent and amount of solvent required). In addition, solubility

data and assessment are the primary determinant of the "mode" of crystallization chosen. Without changes in solubility or the ability to increase solute concentrations above the equilibrium solubility, material will not crystallize from solutions. Frequently used crystallization modes in pharmaceutical production are shown in Table 13.3, along with the solubility behavior that typically leads to the use of each mode. While solubility is important to the initial mode selection, an understanding of kinetics, as described in the next section, is important in defining the parameters required to meet other crystallization objectives, such as particle size and crystalline form.

13.4 CRYSTALLIZATION KINETICS AND PROCESS SELECTION

Solubility, like any thermodynamic relationship, provides a start point and end point for a process. Knowledge of crystallization kinetics is critical in determining the path through which the beginning and end point are linked. For chemical reactions, kinetics are used to indicate the rate of change of molecular species; for crystallizations, kinetics are used to indicate the rate of solute mass transfer from solution phase to a solid phase. While solubility is often a primary control for achieving purification and separation objectives, the kinetic mechanisms of a crystallization are often the primary determinant for physical properties. The discussion below is a simplified description of crystallization kinetics, which are more comprehensively described in several references [1, 3].

Following the preliminary selection of solvent(s) from solubility data, the kinetics of the system must be understood in order to choose the conditions under which the crystallization operates and to validate the choice of solvent(s). If the chosen solvent system presents significant challenges related to kinetics that prevent the crystallization from achieving its design objectives, a new system is often sought.

Essential to understanding the kinetics of crystallization is the concept of supersaturation, which is the driving force for common crystallization mechanisms. Common expressions of supersaturation are shown by the equations presented below, where solubility and concentration units are adjusted for consistency:

$$\text{Supersaturation:} \qquad \sigma_1 = C_{\text{solute}} - S_{\text{solute}} \quad (13.11)$$

$$\text{Supersaturation ratio:} \qquad \sigma_2 = \frac{C_{\text{solute}}}{S_{\text{solute}}} \qquad (13.12)$$

$$\text{Relative supersaturation:} \qquad \sigma_3 = \frac{C_{\text{solute}} - S_{\text{solute}}}{S_{\text{solute}}} = \sigma_2 - 1 \qquad (13.13)$$

In the equations above, C_{solute} is the actual concentration of solute at a temperature or composition condition, S_{solute} is
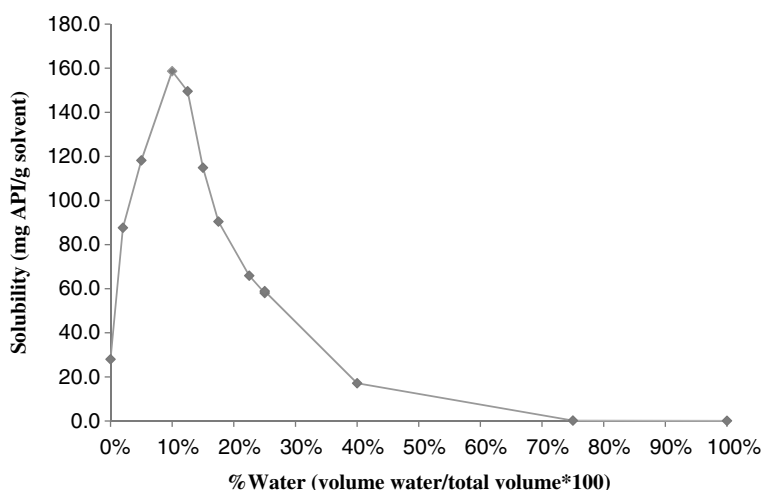
FIGURE 13.13   Solubility enhancement of an API using water as a cosolvent. Water often enhances solubility of pharmaceuticals at moderate concentrations. This particular example uses ethanol as a cosolvent. There is no form change across this water concentration range.

the equilibrium solubility at the same condition, σ_1 is the supersaturation in absolute terms (concentration), σ_2 is referred to as the supersaturation ratio, and σ_3 is referred to as the relative supersaturation. All three terms are frequently used in the analysis of crystallization processes.

Crystal mass formation can be achieved by either nucleation or growth. Nucleation can be described as the formation of new crystals from a solution or slurry, while growth can be defined as the deposition of solute mass on existing crystals of that solute. Nucleation can further be divided into two mechanisms: "primary" nucleation, which is the formation of new crystals from solutions devoid of crystals, and "secondary" nucleation, which is the formation of new crystals in the presence of existing crystals. Primary nucleation can occur within solutions (homogeneously) or at surfaces (heterogeneously), e.g., crystallizer walls and agitators.

Nucleation generates small crystals, which can be useful in preparing small particle size powders. However, nucleation can also lead to significant downstream processing problems such as long isolation times, significant agglomeration leading to poor performance in a formulation, and batch-to-batch variability.

TABLE 13.3   Common Crystallization Modes and the Influence of Solubility Behavior on the Selection of Modes

Crystallization Mode	Description	Solubility Behavior Leading to Mode Selection
Cooling	Crystallization is achieved by cooling solvent from a high temperature to a low temperature at constant solvent composition. Temperature is used to reduce solubility	Compound is soluble in a solvent at an elevated temperature below the normal boiling point of the solvent (e.g., >100 mg/g solvent), but relatively insoluble at a lower temperature (e.g., <20 mg/g solvent)
Antisolvent	Crystallization is achieved by adding an antisolvent to a solvent in which the solute is soluble. Composition is used to reduce solubility	Cooling crystallizations cannot achieve yield constraints (e.g., >90%) at reasonable dilutions (e.g., <20 L solvent/kg compound). The addition of an equal volume of antisolvent to a solvent reduces the solubility of a compound by more than 50%
Reactive	Crystallization is achieved by changing the compound ionically or structurally through reaction. The reactants are often soluble with the product being insoluble. Reaction is used to change the concentration of the product above the solubility limit	The product is completely insoluble in all potential solvents, and the precursors are readily soluble
Evaporative	Crystallization is achieved by the evaporation of solvent that increases the solute concentration above the solubility limit	Often used in combination with a cooling crystallization. For instance, if a cooling crystallization without evaporation can come close to meeting yield requirements, further concentration through distillation will allow additional mass to be recovered

Crystal growth is used to increase the size of the product, reduce batch-to-batch variability, and overcome downstream processing and handling issues [20]. It is also used to control the crystalline form of the compound being prepared, as multiple forms have the potential to simultaneously nucleate. As a result of the benefits afforded by crystal growth, it is generally preferred as the dominant mechanism in crystallization design, especially for controlling physical properties of materials.

13.4.1 Nucleation Kinetics and the Metastable Limit

When solutions are supersaturated, they are thermodynamically unstable. Like chemical reactions that do not react spontaneously, a thermodynamically unstable solution does not necessarily crystallize spontaneously as an energy barrier must be overcome to form a surface, analogous to

the activation energy associated with a chemical reaction. Solutions that are supersaturated but do not spontaneously crystallize are referred to as "metastable." It is quite common for pharmaceutical intermediates and APIs to form metastable solutions at supersaturation ratios between 1 and 1.20. Eventually (i.e., weeks to years), many "metastable" systems might nucleate, but over the timescales associated with processing (i.e., minutes to hours) nucleation typically does not occur. A solute is said to be at its metastable limit when it is at the maximum supersaturation at which primary nucleation does not spontaneously occur.

After solubility, the metastable limit is the next critical measurement in crystallization design. It is measured by two primary methods, which are described in detail in Table 13.4.

An example of metastable limit determination and data reduction is provided by Example 13.4 for a cooling crystallization and an antisolvent crystallization.

TABLE 13.4 Description of Metastable Limit Measurement Techniques

Method	Description
Cooling rate (this method is primarily applicable to cooling crystallizations but can also be applied to evaporative crystallizations)	1. Using solubility data, a saturated solution of compound in solvent is prepared at a temperature close to the maximum temperature of the proposed crystallization in a reactor equipped with a particle measurement device (e.g., turbidity and Lasentec® FBRM®). 2. The solution is cooled at a slow rate (i.e., $\sim 0.1°C/min$) until particles are observed by the measurement device. The temperature at which crystallization is observed is recorded. 3. The experiment is repeated several times at faster cooling rates (e.g., 0.25, 0.5, 0.75, and 1°C/min). 4. A graph is prepared plotting crystallization temperature as a function of cooling rate. This plot should be linear; a linear fit will indicate the nucleation temperature at a 0°C/min cooling rate. 5. The supersaturation at the 0°C/min cooling rate is the metastable limit at this temperature. This limit is often expressed as a temperature difference between the saturation temperature and the temperature estimated at the 0°C/min cooling rate. 6. The experiment can be repeated at lower concentrations. It is best to get additional data at a concentration near the isolation condition. If there is little difference in the metastable limit in supersaturation terms relative to the high concentration point, additional data are not necessary. 7. It is recommended to perform duplicate experiments in the same and different equipment to understand the potential error and variability associated with the measurement. 8. For screening purposes, the observed crystallization temperature at the lowest cooling rate (i.e., 0.1–0.25°C/min) can be approximated as a 0°C/min cooling rate, and the metastable limit estimated from a single measurement.
Nucleation induction time method (this method is applicable to all crystallization types).	1. Saturated solutions of compound are prepared at conditions (temperature and composition) anticipated to be near the starting point of the crystallization. A particle detection probe is inserted (e.g., turbidity or Lasentec® FBRM®). 2. Supersaturation is generated by one of the following methods: (a) cooling the solution as rapidly as possible to a temperature at which the solution is supersaturated; (b) adding nonsolvent to a solvent composition at which the solution is supersaturated; (c) performing a partial reaction to generate supersaturation; or (d) rapidly evaporating a fraction of the solvent. 3. After the rapid generation of supersaturation in step 2, the solution is held isothermally until a particle detection device indicates that particles have formed. The time (i.e., nucleation induction time) to particle formation is recorded. 4. The experiment is performed at multiple conditions (e.g., different temperatures, different amounts of antisolvent added, different amounts of reactants used). 5. The nucleation induction time is plotted as a function of supersaturation. An asymptote will be observed. The supersaturation value at this asymptote is the metastable limit. 6. It is recommended to perform duplicate experiments in the same and different equipment to understand the potential error and variability associated with the measurement.

EXAMPLE 13.4   ESTIMATION OF METASTABLE ZONE WIDTH BY COOLING AND NUCLEATION INDUCTION TIME METHODS

Compound A is to be crystallized through a cooling crystallization in neat ethyl acetate. Compound B is to be crystallized using the addition of *n*-heptane (antisolvent) to a solution of tetrahydrofuran (THF, solvent). For Compound A, the "cooling rate" method is applied, and for Compound B, the nucleation induction time method is used. Here are the data for both studies.

Compound A: A solution of compound A is saturated in ethyl acetate at 65°C. The solubility follows a van't Hoff relationship, with $A_S = -3269.2$ and $B_S = 8.13$ (S_{solute} is in units of g solute/g solvent). The solution is heated to 70°C, and cooled at 0.25°C/min. The crystallization temperature, recorded by turbidity, is 50.4°C. After crystallization, the solution is reheated to 70°C to achieve dissolution, and cooled at 0.5°C/min, with a crystallization temperature of 48.9°C. The procedure is repeated at 0.67°C/min and twice at 1°C/min with crystallization temperatures of 47.3°C, 45.9°C, and 45.4°C, respectively. Estimate the metastable limit of the compound. Report results as supersaturation in units of g solute/g solvent.

Compound B: A solution of compound B is saturated in THF at 20°C. To the THF, different amounts of *n*-heptane (the antisolvent) are added, and the time to crystallization is noted. Relevant data are reported in Table 13.5. Estimate the metastable limit and report as relative supersaturation.

Solution

Compound A: With the data provided, a plot can be made of crystallization temperature as a function of cooling rate. This data can be linearly fit and extrapolated to a 0°C/min cooling rate, illustrated in Figure 13.14a. The extrapolation predicts a crystallization temperature of approximately 52°C at 0°C/min. Estimating the solubility at saturation (65°C) and at a 0°C/min cooling rate (52°C) using equation 13.6 gives

$$S_{solute}(65°C) = e^{\frac{-3269.2}{273.15+65} + 8.13} = 0.215 \text{ g/g solvent}$$

$$S_{solute}(52°C) = e^{\frac{-3269.2}{273.15+52} + 8.13} = 0.146 \text{ g/g solvent}$$

TABLE 13.5   Nucleation Induction Time Data for Compound B

Heptane Volume Fraction	Induction Time (min)	Solute Concentration (g/g solvent)	Solubility (g/g solvent)
0.055	180	0.104	0.0186
0.11	60	0.097	0.0097
0.22	15	0.085	0.0034
0.44	1	0.069	0.0009

(a)

(b)
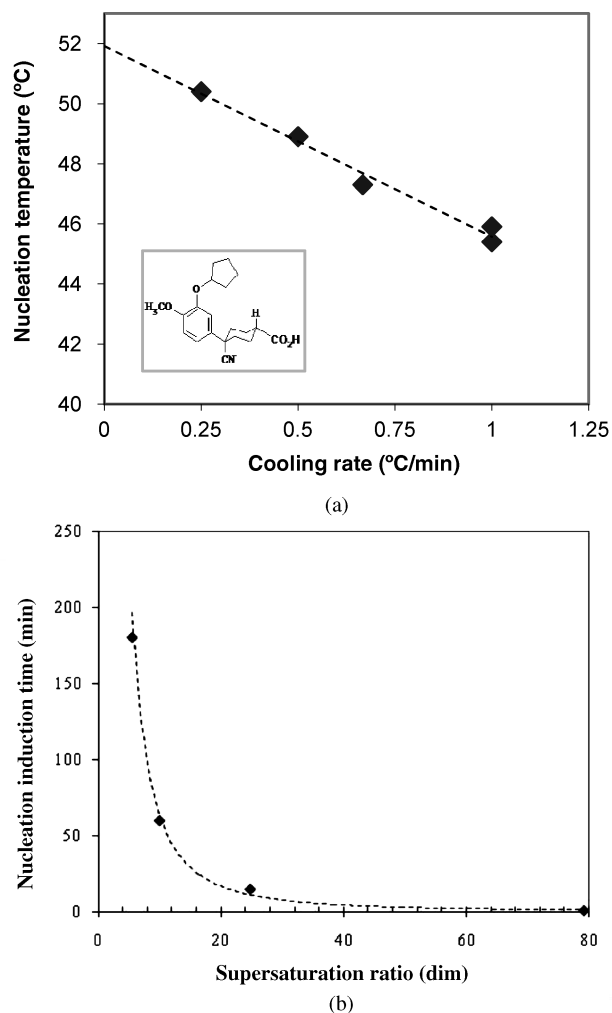
FIGURE 13.14   Metastable zone width measurement using the (a) cooling method for compound A and (b) nucleation induction time method for Compound B. Details are included in Example 13.4.

Then the supersaturation can be calculated for the metastable limit

$$\sigma_1 = 0.215 - 0.146 = 0.069 \text{ g/g solvent}$$

$$\sigma_2 = \frac{0.215}{0.146} = 1.47$$

Compound B: Induction time is plotted as a function of the supersaturation ratio, Figure 13.14b, as calculated from the data in Table 13.5. An asymptote is estimated from a power law fit to the data, giving a superaturation ratio σ_2 of approximately 5. As a result, the relative supersaturation σ_3 is approximately 4.

Of the two methods for estimating metastable zone width, the nucleation induction time method is often the most general, as it is broadly applicable to all crystallization modes. In addition, the nucleation induction time method

gives an indication of the time window that is available to allow the addition and growth of seed materials and mix antisolvents/reactants with the main solution; as a result, it is necessary in understanding the scale-up implications of crystallizations that are described later in this chapter.

While the metastable limit is useful in understanding the conditions under which primary nucleation occurs, the potential for secondary nucleation must also be considered. Secondary nucleation occurs through several mechanisms, with the most common mechanism being contact nucleation. Contact nucleation is microattrition of crystals resulting in small crystalline fragments (i.e., $<10\,\mu m$) being present in the slurry [21]. The rate of contact nucleation is influenced by crystal–crystal, crystal–impeller, and crystal–wall collisions. A common expression for contact nucleation is indicated by equation 13.14:

$$B = k_N M^j N^k \sigma_1{}^b \qquad (13.14)$$

where B is the nucleation rate (number per volume per time), k_N is the nucleation rate constant, M is the suspension density in number (mass per volume), and N is the agitation rate (a frequency or velocity). The variable b is the primary nucleation order and j and k are secondary nucleation orders. Secondary nucleation can occur either within or outside the metastable limit. A simplified version of equation 13.14 (j and $k = 0$) is used to represent primary nucleation kinetics. A thorough treatment of nucleation is provided by Kashchiev in Ref. 22.

13.4.2 Growth Kinetics

Crystal growth theory and mechanisms have been well described [1–3]. For the practicing engineer working on design and scale-up issues, this discussion is simplified below into the content that is typically required to analyze commonly used pharmaceutical crystallization modes.

Like nucleation, crystal growth is driven by a supersaturation driving force, with equation 13.15 illustrating a commonly used rate expression:

$$\frac{dm}{dt} = k_{GM} A_c \sigma_1^g. \qquad (13.15)$$

In the equation above, k_{GM} is a temperature dependent growth rate constant, A_c is the surface area of crystals present in solution, g is the order of growth, and m is the mass of the solid solute. Equation 13.15 is a semiempirical equation merging the serial processes of diffusion of solute to the surface of a crystal and surface integration of solute onto the crystal. Therefore, the parameters k_{GM} and g may also be functions of mixing, as discussed in 13.6. Growth occurs either on material that has already been generated by nucleation or on material that has been purposefully added to the solution. Purposefully added material is referred to as "seed." Seeding is frequently employed in pharmaceutical crystallization processes to control crystalline form and physical properties, especially particle size. Seed material may be prepared from an alternative processing method, such as milling, or may be taken from one batch of material and added to a subsequent batch.

If a system exhibits growth as the primary mechanism for crystal mass formation, the amount and size of seed added control the particle size of the product. A common expression used to interpret the relationship of seed amount to particle size for batch or semi-batch crystallizations is expressed by the proportionality shown below:

$$\frac{m_s}{m_p} \propto \left(\frac{d_s}{d_p}\right)^n \qquad (13.16)$$

In the proportionality, m_s represents the mass of seed, m_p represents the mass of product, and d_s and d_p represent sizes of the seed and product, respectively. Typically, d_{50} or d_{90} values from laser light diffraction measurement or sieve measurement are used for the size terms. The exponent term n is related to the habit of the crystal. For a perfectly spherical crystal, the exponent n would be equal to 3 and the proportionality would be an equality. In practice, the relationship between seed amount and particle size at the end of the crystallization is obtained by an empirical regression of the seed response curve (prepared by running the process at several seed loading (i.e., m_s/m_p) values and trending versus product size for several seed sizes). The preparation of seed response curves and subsequent analysis are listed in Table 13.6.

After regression of the seed response curve, the amount and size of seed required to deliver a desired particle size can be interpolated from the resultant correlations. When conducting these experiments, it is important that supersaturations remain well within the metastable limit, so that growth is the dominant mechanism. An example of a seed response curve is illustrated in Figure 13.15.

In performing seed response curve experiments, the kinetics of crystal growth can also be measured. Growth kinetics are valuable in crystallization design, as they can be used to determine the required rates of cooling, antisolvent addition, distillation, or reagent addition for the corresponding crystallization mode. Many methods for the determination of crystal growth kinetics can be used. A useful method in batch systems is through the measurement of solute concentration as a function of time following the addition of seed to a supersaturated solution. Varying the seed amount changes the "area" term in equation 13.15, allowing the determination of the growth rate constant. The area term is often indicated using a "specific surface area" measurement determined through nitrogen adsorption methods, or by understanding the size distribution of a material and the shape factor through which area of a material can be related to its mass or characteristic length. Measurement of the

TABLE 13.6   Method for Generation of Seed Response Curves

| Step	Description of Step
1	Two to three different types of seed are generated. These may be generated by the following methods: (1) taking existing crystals from the as-is crystallization; (2) taking prepared crystals and performing a particle size reduction step, such as milling, micronization, or sonication (can also be done using a mortar and pestle or a blender); (3) crystallizing material in a different way (e.g., use of other solvents or other modes of crystallization). Each material is measured for particle size by an appropriate technique. The seed loading and seed sizes employed should vary by at least 1 order of magnitude
2	At least three experiments are performed with each seed at different seed loadings. The experiments are performed by seeding within the metastable limit allowing the solution to fully desupersaturate. For the remainder of the crystallization, supersaturation is generated very slowly until the crystallization has reached its completion (i.e., slow cooling rate or antisolvent addition rate). Supersaturation and particle size are monitored to ensure that the mechanism is growth throughout the crystallization
3	The product is isolated and weighed, giving the exact m_s/m_p value. The product is then measured for particle size
4	A seed response curve plots the size of the product versus the seed loading for each different seed size. The particle size as a function of seed loading can be fit through a variety of empirical functions

growth rate constant as a function of temperature enables a growth model over the entire path of a crystallization.

Figure 13.16 displays a typical crystal growth kinetic experiment and associated data fit. For this particular case, an online method (measurement of concentration by reflectance infrared spectroscopy) was used to measure solute concentration. The solute concentration data was used to calculate supersaturation at each time point. The initial conditions for the solution of equation 13.15 were $t = 0$, $C = 0.094$ g solute/g solvent, with the solubility at the experimental temperature ($70°C$) being 0.074 g solute/g solvent (1 L of solvent used with a density of $800\,kg/m^3$). A growth rate order of 1 was assumed. The data was adequately fit through numerical integration using a simple finite differences method and a sum of square residual minimization to estimate a value for $k_{GM} \cdot A_c$ of $1.6 \times 10^{-6}\,m^3/s$. With a seed area of $0.116\,m^2$, $k_{GM} = 1.4 \times 10^{-5}\,m/s$. Due to the relatively small change in mass over the experiment, the value of A_c was approximated to be constant during this experiment. A more rigorous solution would relate mass change to area change through the use of a shape factor and a characteristic seed length, or alternatively an initial rates method would be used with a constant area approximation. Crystallization growth rate orders are often low, with values between 0.5 and 1. In the experience of the authors, a large number of pharmaceutical systems are modeled adequately when assuming first order in supersaturation (i.e., $g = 1$).

13.4.3 Controlling and Determining Crystallization Mechanisms

Figure 13.17 summarizes the kinetic discussions above by displaying regions of concentration in which different mechanisms are likely to occur for either cooling or nonsolvent crystallizations. To maximize the opportunity for crystal growth, operation in close proximity to the solubility is preferred. The nearer the solution concentration is to the metastable limit, the higher the likelihood of secondary nucleation, with primary nucleation possible at concentrations beyond the metastable limit. The principles in Figure 13.17 are also applicable to evaporative and reactive crystallizations, but in these situations supersaturation is typically generated by changes in concentration rather than solubility.
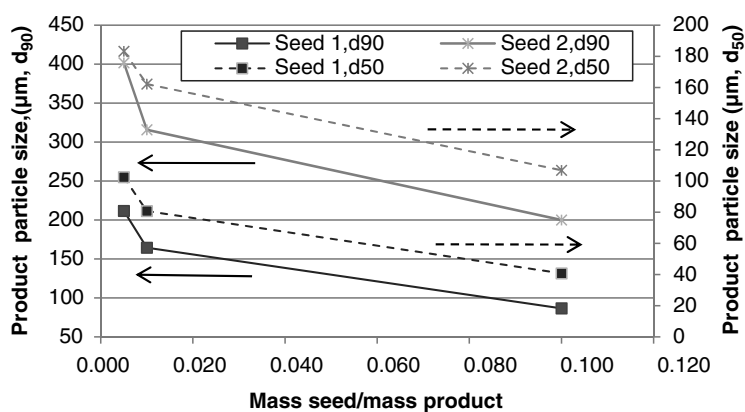

FIGURE 13.15   Typical seed response curve plot. Seed 1 in this case has a d_{90} value of 6.1 μm and a d_{50} of 2.2 μm, while Seed 2 has a d_{90} of 11.5 μm and a d_{50} of 4.4 μm. Both d_{90} and d_{50} values exhibit the anticipated response.
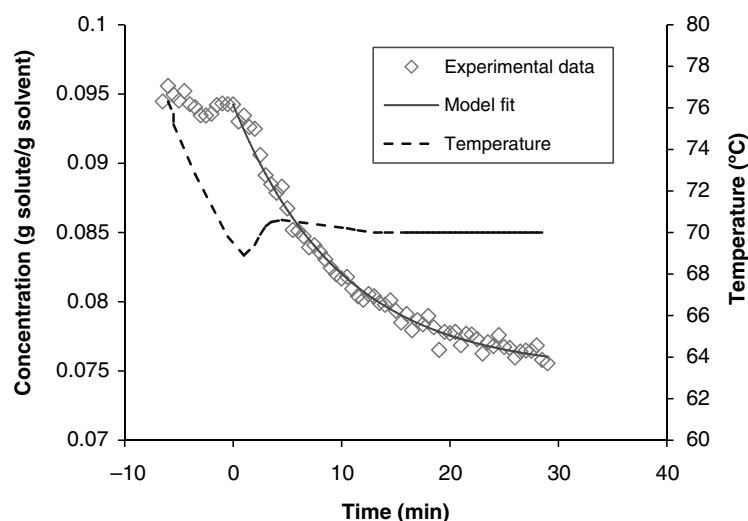
FIGURE 13.16   Crystal growth kinetics from concentration data. Crystallization seeded at time 0. Details are provided in the text. A finite differences approach was used to solve for the growth rate constant, $k_{GM} = 1.4 \times 10^{-5}$ m/s, with seed surface area $A_c = 0.116 \, \text{m}^2$ and solvent volume $V_{solvent} = 1 \, \text{L}$.

Crystallization mechanisms are inferred from experimental data, especially microscopy and solute concentration data. From a design perspective, conditions are sought that provide the balance of mechanisms required to deliver the objectives of the crystallization. In Figure 13.18, successive micro-
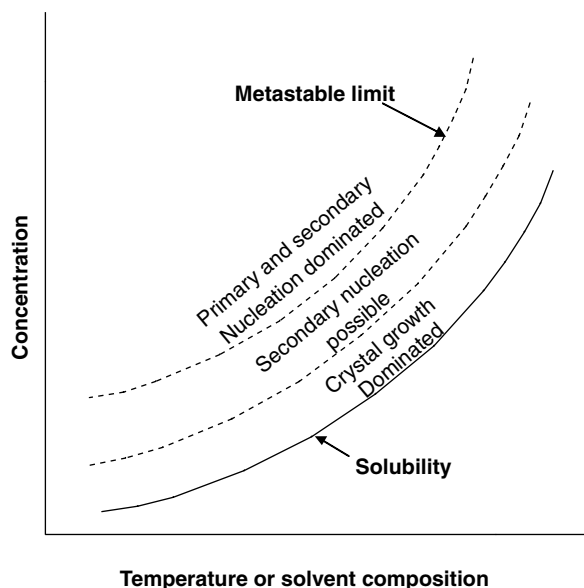

FIGURE 13.17   Mechanisms of crystallization and their relationship to solute concentration. Primary nucleation dominates when the solution is supersaturated beyond the metastable limit. Secondary nucleation can occur within the metastable zone, typically at supersaturations near the metastable limit. Growth frequently is the dominant mechanisms at relatively low supersaturations (i.e., concentration is close to the solubility).

graphs are taken after seeding a pharmaceutical product within the metastable zone. As observed in the figure, the seed materials grow successively larger over time, with no new "fine" crystals observed. This is the type of behavior representative of a growth dominated system and indicates that the crystallization is operating sufficiently close to the solubility curve to minimize secondary nucleation [23].

In Figure 13.19, micrographs are overlaid with solute concentration data for a system that exhibits both growth and secondary nucleation. The solution was supersaturated within the metastable limit before adding seeds. Some crystal growth is observed immediately after seeding. After a growth period where seed material has clearly been enlarged through growth, a change is seen in the slope of the solute concentration curve, indicating a mechanism change from growth to nucleation. Upon further desupersaturation, the crystals have not grown larger and the habit has slightly changed from a columnar habit to more of a thin plate habit while maintaining the same crystalline form. The change in the rate of desupersaturation combined with the change in crystal habit and the lack of crystal enlargement are clear evidence of secondary nucleation.

Of particular use in mechanism detection are process analytical instruments that detect particulate matter, such as in-line microscopy or Lasentec® focused beam reflectance measurement (FBRM®). Overviews of the utility of FBRM® in crystallization mechanism inference can be found in other references [24].

When considering a design for a crystallization that favors growth, a recommended starting point for a design is to seed at a solution concentration no more than midway between the solubility curve and the metastable limit, and
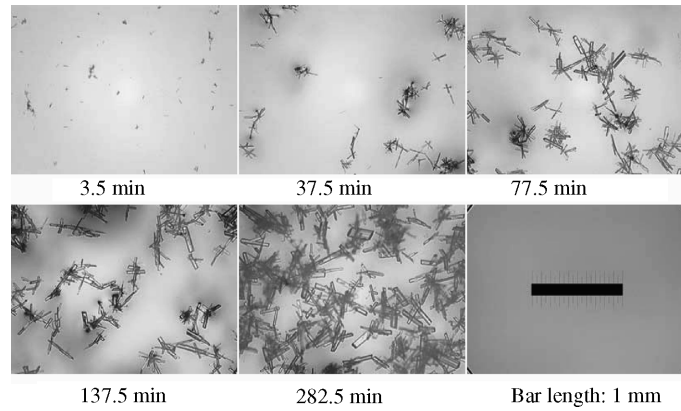
FIGURE 13.18 Illustration of crystal growth mechanism observed by optical microscopy. The process is seeded at time 0 and held isothermally for 282.5 min. Fine particles disappear as coarse particles appear, which grow larger throughout the duration of the experiment with no evidence of fines reappearance [18].

to maintain this minimum proximity to the solubility curve for the remainder of the crystallization process. Initial experiments are performed using microscopy, concentration, and online particle detection methods to ensure the selected conditions are indeed producing the desired mechanism. Conditions are then verified at larger scale to ensure that changes in mixing or equipment geometry and materials of construction have not altered the mechanistic behavior. Acicular habits, in particular, are highly prone to contact nucleation as they can easily be broken. Changes in scale can change the rate of secondary nucleation due to changes in agitation.

In addition to growth and nucleation, oiling, aggregation, and agglomeration are also potential phenomena in crystallization. In the case of oiling, supersaturation is typically in great excess of the metastable limit, or the solution is sufficiently concentrated with nucleation inhibiting impurities. As a result the solute forms a liquid phase consisting of a solvent–solute concentrate rather than a stable crystalline form. Oils are metastable and may crystallize spontaneously with sufficient holding times. Oiling is often prevented through seeding or by nucleation at low supersaturation; if this approach is unsuccessful, impurities must be individually
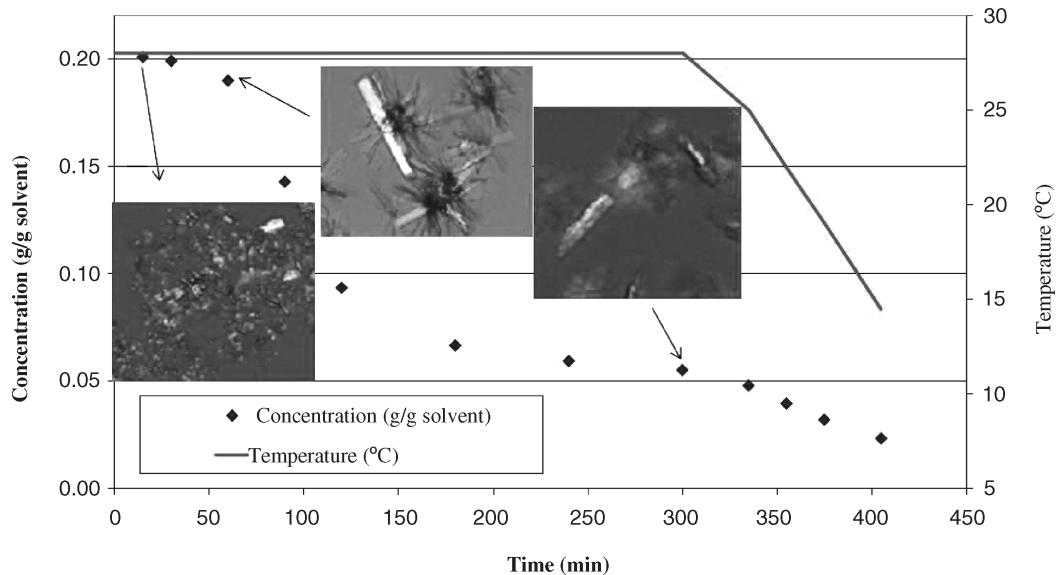
FIGURE 13.19 A crystallization experiment exhibiting both growth and secondary nucleation mechanisms. Initially, seeds grow as indicated by the presence of large crystals shortly after seeding. With additional time, a change in slope during desupersaturation is observed, indicating a change in mechanisms to secondary nucleation.

investigated for their inhibition of nucleation and growth, with the problematic impurity removed by alternative means.

Aggregation occurs when two crystals collide in solution and adhere to each other through favorable surface-surface interactions. Once an aggregate forms, it can either be "deaggregated" with crystals regaining their individual identity (this typically occurs through fluid shear), or the crystals may fuse together due to growth which links the two surfaces. When crystals fuse together, the result is called an agglomerate. Aggregation is often severe in processes in which nucleation occurs at high supersaturations, and is common for acicular habits or for crystals with high specific surface areas. Severe aggregation is often manifested as an immobile slurry that does not mix well and under certain conditions can form "shelves" of solid material on internal reactor equipment. As aggregation and agglomeration can affect processability, physical properties and mixing scale-up, the approach is often taken to minimize supersaturation to reduce the driving force for aggregate and agglomerate formation. When formed, agglomerates often cause bimodal size distributions and batch-to-batch variability in products. Because agglomeration is difficult to scale-up and control, it is often avoided as a selected mechanism.

In certain instances, aggregation or agglomeration are purposefully attempted to prepare a material that behaves like a small particle from a pharmaceutics perspective (e.g., rapid dissolution in a dosage form) but behaves like a larger particle from a manufacturability perspective (e.g., short filtration times). Examples of the favorable use of aggregates or agglomerates include spherical crystallizations [25]. The design of a spherical crystallization process is highly dependent on the properties of a molecule, and often must be established on a trial and error basis.

13.5 UNDERSTANDING CRYSTALLIZATION RATE PROCESSES: THE APPLICATION OF SOLUBILITY AND KINETICS DATA TO CRYSTALLIZATION MODES

The kinetic and thermodynamic principles described in the previous sections can be applied to common crystallization modes to complete a design. For most situations, it is recommended to pursue a design where growth is the dominant mechanism, as such processes are simpler to reproducibly scale-up from a heat and mass transfer perspective. To enable a growth basis for design, seeding is employed to provide the initial area required for growth. This is especially the case for active ingredients where control of particle size and crystalline form are key objectives. When tight control over physical properties is less of an issue, a preferred design approach may be to nucleate at a consistent, small supersaturation (i.e., just outside of the metastable limit), and then

grow the nuclei at a supersaturation within the metastable limit.

These two design methods are illustrated in Figure 13.20 for common crystallization modes. In Figure 13.20b, d, and f, the crystallization is seeded within the metastable limit and supersaturation is maintained within the metastable limit until the crystallization has completed. This approach provides the best opportunity to maximize the potential for crystal growth. In Figure 13.20a, c, and e, nucleation is induced by increasing the supersaturation beyond the metastable limit, but supersaturation is then controlled to ensure that the rest of the crystallization occurs close to the solubility line.

A common error in crystallization design and scale-up is the generation of supersaturation to levels where nucleation is a dominant mechanism. This is caused by a lack of understanding of the timescales over which controlling process parameters need to be changed. This section addresses simple approaches to estimating the timescales for the controlling parameters in each major crystallization mode:

- Rate of temperature change (cooling crystallizations)
- Rate of addition of antisolvent (antisolvent crystallizations)
- Rate of reaction through control of temperature or addition of reactants (reactive crystallizations)
- Rate of solvent removal (evaporative crystallizations)

Only simple methods for the estimation of timescales and rate processes for batch or semi-batch crystallizations are described. There are many published examples of more rigorous approaches to solving similar problems, particularly the work of the Bratz [26] and Rawlings [27] research groups, which are recommended for further study. In particular, more detailed modeling approaches using partial differential equations and the method of moments as a solution of the population balance equation are encouraged. More detailed information regarding the use of population balances to model crystallization processes is provided in the literature [28].

13.5.1 Cooling Crystallization

Seeded, cooling crystallizations represent perhaps the simplest design approach for achieving consistent crystallizations while minimizing scale-up challenges. The design challenge is to balance the crystal growth rate with the rate of supersaturation generation. In order to understand the required rate of change of temperature to meet this objective, a knowledge of crystal growth kinetics for the seed material is required (Figure 13.16).

To estimate the rate of temperature change for a cooling crystallization design, the crystal growth rate is balanced with the rate of supersaturation generation through cooling
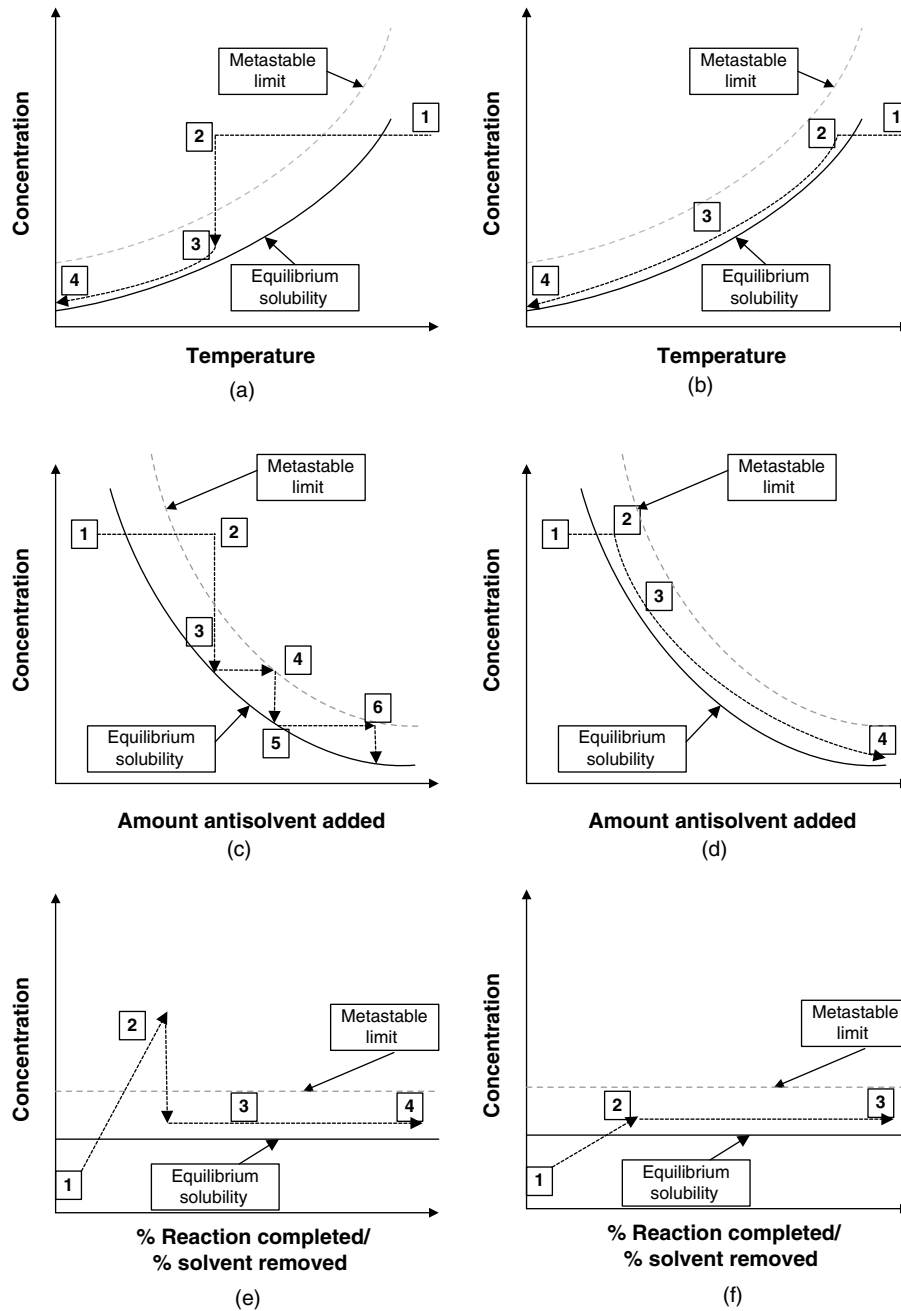
FIGURE 13.20   Frequently used crystallization design modes in pharmaceutical processes. (a) and (b) represent cooling crystallizations, (c) and (d) represent crystallizations induced by antisolvent addition, and (e) and (f) represent both reactive and evaporative crystallizations, which can be similar in terms of behavior. (a), (c), and (e) represent situations where initial crystal mass is generated by primary nucleation, with growth occurring after the nucleation event through controlled generation of supersaturation. The amount of nucleation is dependent on how much supersaturation is generated prior to crystallization. (b), (d), and (f) represent seeded crystallizations, where seed is added in the metastable zone. In each plot, [1] represents the starting point of the crystallization, where all material is dissolved [2] represents the point at which crystallization mass is first generated, either by seeding or by nucleation. The highest number on each plot represents the point at which the crystallization is complete.

such that the process remains within the metastable limit and near the solubility line. A simple approach to achieving this is through the evaluation of equation 13.17, where the growth rate is expressed both in terms of the solid phase (dm/dt) and the solution phase ($V_{solvent}(dC_{solute}/dt)$), and the solution phase concentration is constrained to a constant supersaturation, σ_1:

$$\frac{dm}{dt} = -V_{solvent}\frac{dC_{solute}}{dt} = k_{GM}A_c\sigma_1^g \cong -V_{solvent}\frac{\Delta C_{solute}}{\Delta T}\frac{\Delta T}{\Delta t}$$

where $C_{solute} = S_{solute} + \sigma_1$ and σ_1 is constant during cooling

(13.17)

Through knowledge of the metastable limit and nucleation induction times, a supersaturation is first selected at which the material is desired to grow. Typically, this is a concentration within the metastable limit and close to the solubility line. The exact value selected is dependent on the compound and its propensity for secondary nucleation within the metastable limit. Care must be taken to not dissolve seed material due to process variability. For instance, if a solution is saturated at 70°C, and the selected seeding temperature is at 68.5°C, but the temperature probe has an error of 2°C and the solvent charge has an error of 1%, the seeds may dissolve. A commonly employed seeding method involves seeding at a supersaturation within the metastable limit but at a level where the typical processing errors that can cause seed dissolution are highly improbable. After seed growth desupersaturates the solution to an acceptable level, further supersaturation generation can be achieved through cooling.

Equation 13.17 and its variations can be solved with simple numerical solutions to determine both the time required for seed to desupersaturate a solution through growth and the cooling rates after the initial desupersaturation. This is illustrated in Example 13.5.

EXAMPLE 13.5

A cooling crystallization is being planned for an API in 1 L of solvent. The solubility (g solute/g solvent) of the compound in question can be modeled using a simple van't Hoff expression with $A_S = -3773.0$ and $B_S = 8.3930$. The starting concentration for the crystallization is 0.0952 g solute/g solvent, and the density of the solvent is 800 kg/m³. A seeding temperature of 70°C is selected with the same area of seed as used in the kinetics experiment illustrated in Figure 13.16 (0.116 m²). After the solution has reached a supersaturation $\sigma_1 = 0.002$ g solute/g solvent, the solution is cooled to 0°C at a constant supersaturation (0.002 g solute/g solvent). Using the kinetic constant and seed area from Figure 13.16, and assuming that $k_{GM} \cdot A_c$ is constant throughout the crystallization, answer the following questions:

1. What is the amount of time required for the seed to desupersaturate the solution to a supersaturation $\sigma_1 = 0.002$ g/g solvent at the seeding temperature, 70°C?
2. What is the minimum time it will take to cool the slurry to 0°C, maintaining a supersaturation $\sigma_1 = 0.002$ g/g solvent throughout the crystallization?

Solution

The first question can be answered using a simple finite differences solution to equation 13.17:

$$\frac{dm}{dt} = -V_{solvent}\frac{dC_{solute}}{dt}$$

$$= k_{GM}A_c\sigma_1^g \Rightarrow \Delta C_{solute} = -\frac{k_{GM}A_c\sigma_1^g}{V_{solvent}} \cdot \Delta t$$

The van't Hoff relationship for solubility, equation 13.6, is used to calculate the saturation concentration of the compound at 70°C:

$$S_{solute}(70°C) = e^{\frac{A_S}{T}+B_S} = e^{\frac{-3773.0}{70+273.15}+8.3930}$$

$$= 0.0741 \text{ g/g solvent}$$

This allows a calculation of supersaturation at the seed addition, time 0:

$$\sigma_1(0) = 0.0952 - 0.0741 = 0.0211 \text{ g/g solvent}$$

And the corresponding finite change in concentration at time 0, picking a suitable time step, here 1 min for illustration purposes:

$$\Delta C_{solute}(0 \text{ min}) = -\frac{k_{GM}A_c}{V_{solvent}} \cdot \sigma_1^g \cdot \Delta t$$

$$= -\frac{1.40 \times 10^{-5} \text{ m/s} \cdot 0.116 \text{ m}^2}{1.00 \times 10^{-3} \text{ m}^3}$$

$$\times (0.0211 \text{ g solute/g solvent})^1 \cdot 60 \text{ s}$$

$$\Delta C_{solute}(0 \text{ min}) = -0.0021 \text{ g/g solvent}$$

Then the concentration, supersaturation, and change in concentration at time 1 min can be calculated:

$$C_{solute}(1 \text{ min}) = 0.0952 - 0.002 = 0.0930 \text{ g solute/g solvent}$$

$$\sigma_1(1 \text{ min}) = 0.0930 - 0.0741 = 0.0189 \text{ g solute/g solvent}$$

$$\Delta C_{solute}(1 \text{ min}) = -\frac{1.40 \times 10^{-5} \text{ m/s} \cdot 0.116 \text{ m}^2}{1.00 \times 10^{-3} \text{ m}^3}$$

$$\times (0.0189 \text{ g solute/g solvent})^1 \cdot 60 \text{ s}$$

$$= -0.00184 \text{ g solute/g solvent}$$

This sequence can be continued until reaching the desired supersaturation, $\sigma_1 = 0.002$ g/g solvent. This would most
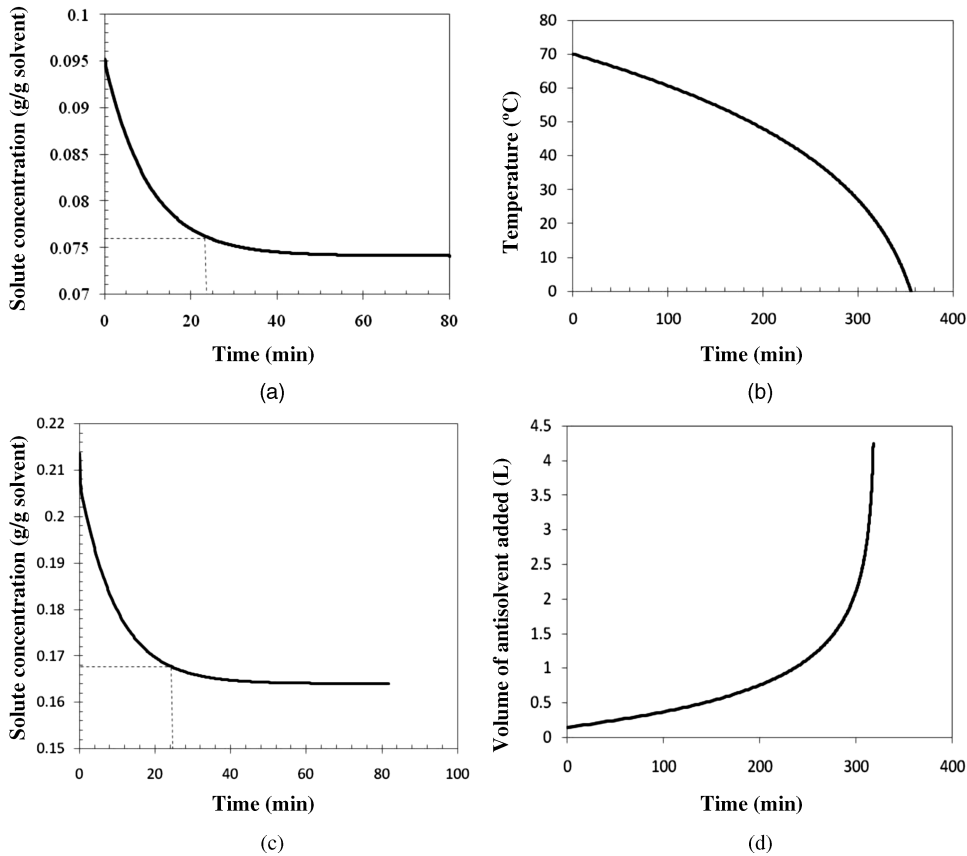
FIGURE 13.21 Calculated crystallization timescales and rate changes for a cooling crystallization (a) and (b) and an antisolvent addition (c) and (d). The cooling crystallization is described by Example 13.5, and the antisolvent example is described in the text. For (a) and (b), $k_{GM} \cdot A_c =$ constant $= 1.6 \times 10^{-6} \, \text{m}^3/\text{s}$ and $A_c = 0.116 \, \text{m}^2$. The solubility was represented by a simple van't Hoff correlation with $A = -3773.0$ and $B = 8.390$, and the solvent volume was 1 L. Seeding was performed at 70°C, with the criteria that a supersaturation, σ_1, of 0.002 g/g solvent be reached during isothermal seed growth (a), and with that value maintained during cooling (b). For (c) and (d), $k_{GM} \cdot A_c =$ constant $= 1 \times 10^{-5} \, \text{m}^3/\text{s}$, with $A_c = 0.71 \, \text{m}^2$. The initial volume of methanol was 6 L, with 0.15 L water added to supersaturate. Seed was isothermally grown until a supersaturation of 0.004 g/g solvent was achieved (c), and then the balance of water, 4.1 L, was added isothermally while maintaining this supersaturation (d).

easily be completed in a spreadsheet, and smaller time steps would improve accuracy. The solution to this is illustrated in Figure 13.21a and the time required is approximately 24 min using a 0.2 min time step.

For the second question, the challenge is to crystallize at a constant supersaturation that constrains the growth rate to a constant value for the entire crystallization. Starting from the end of the last example, a finite differences approach is again applied. Using the starting point as a concentration of 0.0761 g/g solvent, and a constant growth rate as defined by $k_{GM} \cdot A_c \cdot \sigma_1$, the temperature is stepped in suitable ΔT increments to the end temperature, 0°C. The solubility is then calculated at each ΔT increment, and the supersaturation is added to the solubility at the ΔT increment to give the

solution concentration at this time point, and a ΔC_{solute} from one temperature to the next. The time, Δt, is calculated for each ΔT interval by dividing ΔC_{solute} by $k_{GM} \cdot A_c \cdot \sigma_1/V_{solvent}$. The time at each temperature is estimated by cumulatively adding the Δt values. This is illustrated below where $\Delta T = 1.0°C$:

$$T_1 = 70°C; \ S_{solute}(70°C) = e^{\frac{A_S}{T} + B_S}$$

$$= e^{\frac{-3773.0}{70 + 273.15} + 8.3930} = 0.0741 \text{ g solute/g solvent}$$

$$C_{solute \ T_1} = S_{solute \ T_1} + \sigma_1 = 0.0741 + 0.002$$

$$= 0.0761 \text{ g solute/g solvent}$$

$$T_2 = 69°C; \ S_{\text{solute}}(69°C) = e^{\frac{A_S}{T} + B_S}$$

$$= e^{\frac{-3773.0}{69 + 273.15} + 8.3930} = 0.0718 \text{ g solute/g solvent}$$

$$C_{\text{solute } T_2} = S_{\text{solute } T_2} + \sigma_1 = 0.0718 + 0.002$$

$$= 0.0738 \text{ g solute/g solvent}$$

$$\Delta t_1 = \frac{[C_{\text{solute } T_1} - C_{\text{solute } T_2}]}{k_{\text{GM}} A_c \sigma_1} V_{\text{solvent}}$$

$$= \frac{(0.0761 - 0.0738) \text{ g solute/g solvent}}{1.40 \times 10^{-5} \text{ m/s} \cdot 0.116 \text{ m}^2 \cdot 0.002 \text{ g solute/g solvent}}$$

$$\cdot 1.00 \times 10^{-3} \text{m}^3 = 722 \text{s}$$

For each subsequent temperature interval, a new time interval is then calculated in a similar manner and time is cumulatively added until the end crystallization temperature, 0°C, is reached.

From this analysis a plot of T versus t can be produced. The total calculated crystallization time is approximately 355 min, with the profile shown in Figure 13.21b. As observed in Figure 13.21b, the rate of temperature change increases at lower temperatures. This is because the solubility rate of change at high temperatures is greater than at low temperatures. Because of the constant $k_{\text{GM}} \cdot A_c$ assumption, this time is a conservative estimate. A more rigorous solution would update A_c as a function of the change in crystal mass, m, through the use of shape factors that relate the area of a crystal to its volume and a characteristic length.

In the event that seeding is not practical (e.g., for the crystallization of intermediates) an alternative approach is to cool to a temperature outside of the metastable limit, nucleate at a selected supersaturation, and then control the subsequent cooling in order to maximize crystal growth. The same methodology shown in Example 13.5 is applicable for the subsequent growth phase, except that the nucleated material must have an estimated area in order to apply a growth kinetic model.

An often used methodology in cooling crystallizations is the performance of a "ripening" step to increase particle size and improve downstream unit operations (e.g., isolation). Ripening involves reheating a slurry to partially dissolve some of the crystal mass (typically at least 10% of solids remain undissolved) and then recooling to promote growth on the remaining crystals (fines will typically dissolve first as dissolution rate is proportional to the surface area to volume ratio of a particle [6]). Ripening is frequently employed when nucleation is a significant mechanism due to slow crystal growth rates, and is a way to provide a large area for growth without initially adding large amounts of seed material (i.e., >10%).

13.5.2   Antisolvent Crystallization

The rate of antisolvent addition to maximize growth potential can be calculated through a similar approach to that described for a cooling crystallization. In this case, the volume is not constant but varies over time, resulting in equation 13.18:

$$\frac{dm}{dt} = -\frac{d\{(V_{\text{solvent}} + V_{\text{antisolvent}})C_{\text{solute}}\}}{dt} = k_{\text{GM}} A_c \sigma_1^g$$

where $C_{\text{solute}} = S_{\text{solute}} + \sigma_1$ during antisolvent addition

(13.18)

To maintain the equality in equation 13.18, the antisolvent addition rate will often be slow initially and will increase near the end of the crystallization. However, the addition rate profile is highly dependent on the shape of the solubility curve [29]. As with a cooling crystallization, the first step is to add antisolvent to generate a supersaturation within the metastable limit, and then calculate the time needed to desupersaturate for a given seed load. This is accomplished through a numerical solution of equation 13.18, knowing $k_{\text{GM}} \cdot A_c$, the temperature, and the composition (the solution is similar to the first question in Example 13.5).

After desupersaturating the solution through seed growth at a constant composition, the next step is to calculate the rate of antisolvent addition. This can be achieved through a numerical integration of equation 13.18. It is first necessary to select a supersaturation appropriate to maintain crystal growth using metastable limit data. A simple finite difference approach involves starting at this supersaturation, σ_1, and calculating the growth rate, $k_{\text{GM}} \cdot A_c \cdot \sigma_1^g$. The volume is then incremented in small intervals, with the change in solute mass (Δm_{solute}) calculated over each volume interval ($V_{n+1} - V_n$) through the difference of the solubility times the mass of solvent across the volume interval:

$$\Delta m_{\text{solute}} = -\{(V_{\text{solvent}} + V_{\text{antisolvent}_{n+1}}) \cdot S_{\text{antisolvent}_{n+1}}$$
$$-(V_{\text{solvent}} + V_{\text{antisolvent}_n}) \cdot S_{\text{antisolvent}_n}\}$$

The time required for each added increment of antisolvent, Δt, is calculated by dividing the change in solute mass by the calculated growth rate.

The results of antisolvent crystallization calculations are shown in Figure 13.21c and d for a system in which water is added to a methanol solution containing an API, assuming that $k_{\text{GM}} \cdot A_c$ is constant over the entire crystallization (i.e., 1.0×10^{-5} m^3/s) with a growth order of 1. For this particular scenario, the solvent is methanol and the antisolvent is water, and the solvents are assumed to mix ideally. The solubility of the binary system is described by an exponential function, $S_{\text{solute}} = 0.22 \exp(-12.04 \ \phi_{\text{water}})$ g solute/g solvent, where ϕ_{water} is the water volume fraction. Initially, 1 kg of material is dissolved in 6 L of methanol, and 0.15 L of water is added to generate supersaturation at 20°C. The solution is then seeded and held until a supersaturation of 0.004 g/g solvent is

achieved. Antisolvent is then added at a rate such that this supersaturation is maintained to achieve a total added volume of 4.25 L. The result is a seed hold time of approximately 24 min and a total addition time of approximately 317 min. The shape of the addition curve mirrors the solubility as a function of water volume fraction. As with the cooling crystallization, nucleation can also be used to initiate the crystallization, with growth rates calculated after estimating the area generated in the nucleation step.

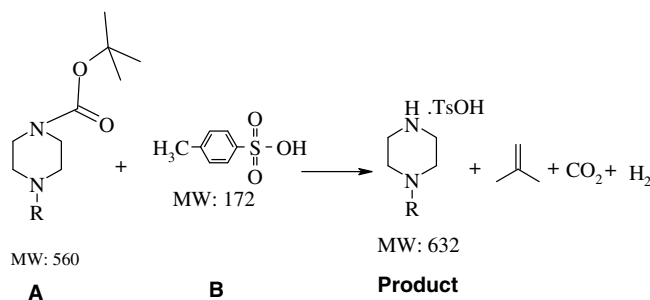### 13.5.3   Reactive Crystallization

In most cases, reactive crystallizations are of interest when the product of the reaction is sparingly soluble and the crystallization rate is slow compared with the reaction rate. For these systems, the challenge is to match the rate of product generation with the rate of crystal growth so that excess supersaturation is not generated. For a simple bimolecular reaction, where {A + B → Product}, the following rate balance can be written:

$$\frac{dm_{\text{product}}}{dt} = MW_{\text{product}}k_{\text{reaction}}[A][B]V_{\text{solvent}} = k_{\text{GM}}A_c\sigma_1^g$$

$$(13.19)$$

The rate of reaction for many pharmaceutical applications can be controlled by the rate of addition of reactant, resulting in the volume (V_{solvent}) being a function of addition rate and time. In the simplest instance, the reactant of interest is an ionizable compound that forms a salt with the pharmaceutical molecule, with the molecule then having a negligible solubility in the solvent (typically a solvent with low polarity). In this situation, the rate of reaction is essentially instantaneous with the addition of the reactant (B), and the left hand side of equation 13.19 becomes

$$\frac{dm_{\text{product}}}{dt} = -\frac{d[V_{\text{B,f}}C_{\text{B,f}}]}{dt}\frac{MW_{\text{product}}}{MW_B}$$

where f represents the feed solution in which reactant B is contained. This solution is similar to that shown for antisolvent crystallization.

FIGURE 13.22   Reaction scheme as an example of a reactive API crystallization process.

An example of a common pharmaceutical synthesis reaction is shown in Figure 13.22. This is a "Boc" deprotection reaction with an acid reactant. Upon deprotection, the resultant species is able to form a salt, which has limited solubility in the reaction solvent. A numerical solution to equation 13.19 is illustrated in Figure 13.23a for this example, which shows that the concentration of B must increase as a function of time to maintain constant supersaturation. This increase is required to maintain a constant reaction rate with [A] that is decreasing due to consumption. Conditions used are provided in Figure 13.23a.
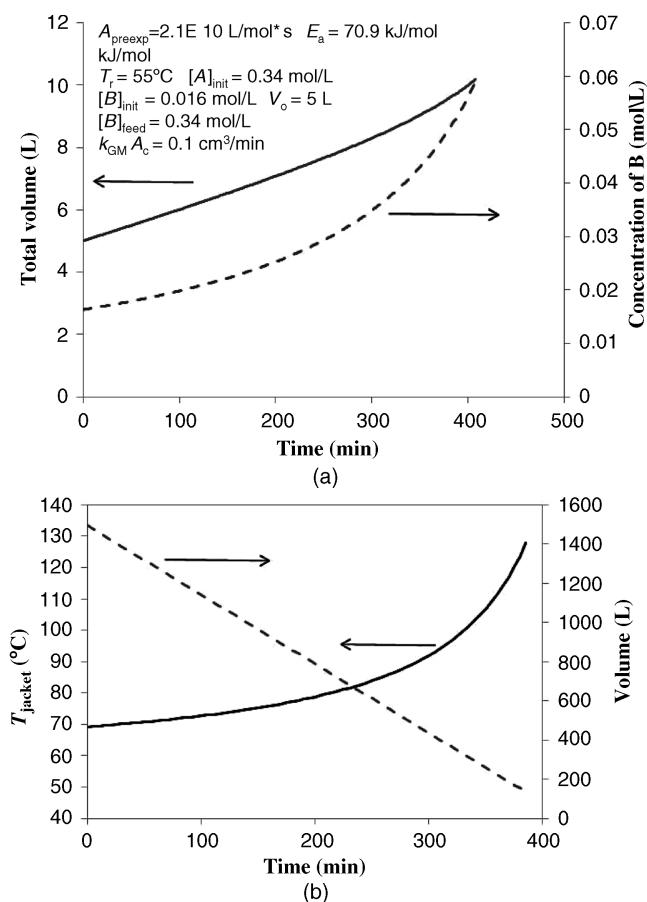
A common problem in reactive crystallization is the presence of impurities in the final product at levels higher than predicted from solubility data. This can occur for two reasons. First, the impurity may be structurally similar to the desired molecule, and thus able to form some of the same bonding arrangements in the lattice. As a result, the impurity is integrated into the crystal. For reactive crystallizations, the reactant molecule is often similar in structure to the desired product, so integration is a distinct possibility. The second cause is referred to as inclusion, and occurs due to crystallization liquors being trapped into the crystal lattice as it forms or grows. Inclusion is more prone to occur when liquors are highly viscous or when crystal formation and growth kinetics are rapid. If impurities that are soluble in a wash solvent are not able to be effectively washed from surfaces, either inclusion or integration is the likely cause.

13.5.4   Evaporative Crystallization

In evaporative crystallization, the solubility is constant, so the rate of supersaturation generation is proportional to the rate of solvent mass removal (dm_{solvent}/dt)

$$\frac{dm}{dt} = S_{\text{solute}}\frac{dm_{\text{solvent}}}{dt} \cong S_{\text{solute}}\frac{U \cdot A_{\text{vessel}}(T_j - T_r)}{\Delta H_v} = k_{\text{GM}}A_c\sigma_1^g$$

$$(13.20)$$

In equation 13.20, U is the overall heat transfer coefficient of a batch reactor, A_{vessel} is the heat transfer area, and ΔH_v is the heat of vaporation of the solvent. The heat of crystallization is not included as it is often negligible relative to the heat transferred through vessel walls for batch crystallizations. A constant evaporation rate is necessary to maintain a constant crystal growth rate at a constant supersaturation and the evaporation rate is balanced with the crystal growth rate. The controlling variable in the determination of the evaporation rate is the jacket temperature of the reactor, T_j. As the volume decreases in the reactor, the effective heat transfer area decreases, thereby changing the temperature required on the jacket to maintain the constant evaporation rate. A sample calculation for T_j estimation during an evaporative crystallization is illustrated in Figure 13.23b. In practice, the T_j values shown in Figure 13.23b toward the

A_{preexp}=2.1E 10 L/mol*s E_a = 70.9 kJ/mol kJ/mol
T_r = 55°C $[A]_{init}$ = 0.34 mol/L
$[B]_{init}$ = 0.016 mol/L V_o = 5 L
$[B]_{feed}$ = 0.34 mol/L
$k_{GM} A_c$ = 0.1 cm³/min

(a)

(b)

FIGURE 13.23 Examples illustrating constant supersaturation control for (a) reagent addition for a reactive crystallization and (b) jacket temperature for an evaporative crystallization. The reaction for (a) is shown in Figure 13.22, run isothermally at 55°C ($E_a = 70.9$ kJ/mol, $A_{preexp} = 2.1 \times 10^{10}$ L/mol s). Starting amount of compound A is 1 kg in 5 L solvent. Initially, the reaction was run to approximately 5% completion, through an addition of 5 mol% compound B, and a product concentration of 0.004 g/g solvent was achieved after seeding and seed growth. The balance of B was then added in a feed solution with a concentration of 0.336 mol/L. Compound B was added such that a supersaturation of 0.004 g/g solvent was maintained. $k_{GM} \cdot A_c = $ constant $= 9.8 \times 10^{-6}$ m³/s. For (b), the solvent was distilled from 1500 to 100 L; $k_{GM} \cdot A_c = $ constant $= 2.9 \times 10^{-4}$ m³/s. The vessel has a linear correlation between surface area and volume A_{vessel} (m²) $= 0.00322 V_{solvent} + 0.53$. The overall heat transfer coefficient was 340 W/m² K, the solvent was methanol, and the supersaturation upon seeding was 0.005 g/g solvent; this was maintained throughout the crystallization.

end of the crystallization would not be used out of concern for material degradation. As a result, the crystallization would simply have a maximum allowed jacket temperature and proceed at a slower rate.

13.5.5 Continuous Crystallization

Continuous crystallization, though not historically used in pharmaceutical processing due to low production volumes and a batch manufacturing infrastructure, has recently gained attention as a way to reduce batch-to-batch variability and minimize solvent waste. A common "model" used for a continuous crystallizer is the mixed suspension, mixed product removal crystallizer, in which the same number of crystals entering the system leaves the system simultaneously. The crystals that leave the system will have grown commensurate with the growth rate, or nucleated if the system is sufficiently supersaturated. If, similar to the analysis above, the system is seeded immediately prior to entering the crystallizer, the resulting crystal growth can idealistically be modeled by the following combination of equations. Equation 13.21 relates crystal mass with its characteristic length [30]:

$$m = aL^3 \rho_M \tag{13.21}$$

where L is the characteristic crystal length, a is a proportionality constant relating the volume of a crystal to its characteristic length, and ρ_M is density of the crystal. Differentiating equation 13.21 and utilizing the growth rate structure introduced in equation 13.15, equation 13.22 provides a highly idealized approach to determine the growth of crystals:

$$\frac{dm}{dt} = 3aL^2 \rho_M \frac{dL}{dt} = k_{GM} A_c \sigma_1^g \tag{13.22}$$

Then over the average residence time of a particle in a continuous crystallizer, the growth can be approximated with equation 13.23:

$$\Delta L = \frac{k_{GM} A_c \sigma_1^g}{3aL^2 \rho_M} \tau \tag{13.23}$$

where τ is the mean residence time of a particle in the crystallizer, σ_1 represents the average supersaturation in the vessel, and ΔL represents the average change in the characteristic length for the particles across the vessel.

13.5.6 Statistical Experimental Design Methods

Factorial experimental designs have rightfully gathered substantial support recently in the pharmaceutical development field. As illustrated by the methodology provided for solubility measurement, seed response curve generation, and crystal growth rate estimation, a semi-empirical, mechanistic-based approach to crystallization design is preferred over a factorial design approach, due to the likelihood of crystallization mechanism change across wide experimental designs. Factorial designs are usefully applied to the robustness evaluation of process factors such as input quality, seed amount, and temperature variations. In robustness studies,
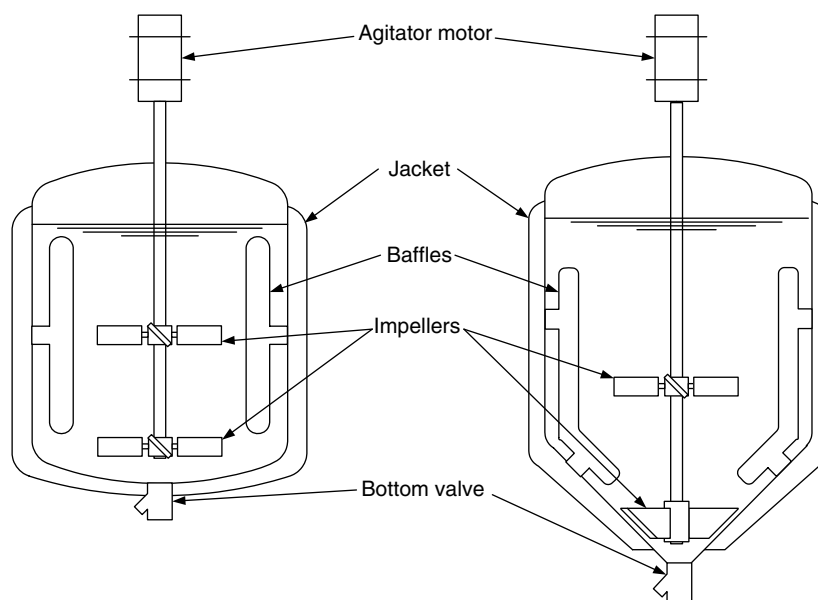
FIGURE 13.24   Schematics of typical vessel designs.

these variables are changed over intervals where the crystallization mechanism is likely to remain the same as the base design condition, so that the variance of a response to common scale-up perturbations can be well understood.

13.6   BATCH CRYSTALLIZATION SCALE-UP

In order to select appropriate scale-up parameters, crystallization scale-up involves understanding a system's relative sensitivities to heat and/or mass transfer [31]. Batch operation is the standard for much of the pharmaceutical industry, therefore stirred-tank reactors are the most commonly available equipment for crystallizations. Reactors are offered by many manufacturers and in several configurations. While they may be purpose-built for a process, they are usually built as multiuse reactors to offer the most flexibility for production. There are two common vessel designs for multipurpose batch reactors—both utilizing a cylindrical tank but having either a dish or conical bottom, as illustrated in Figure 13.24. Agitation designs, including impellers and

baffles, vary widely. Independent of the reactor design, the two primary considerations for crystallization equipment scale-up are heat transfer and mixing.

13.6.1   Heat Transfer Considerations

Heat transfer for reactors is usually achieved by circulating heat transfer fluid (e.g., water, steam, or silicon-based fluids) through an external jacket or heating coils (Figure 13.25). External jackets are the most common for the multiuse reactors typically encountered, and for conventional vessel designs the reduced heating surface area to volume ratio on scale-up significantly reduces the heat transfer capacity, as illustrated by Example 13.6.

EXAMPLE 13.6   HEAT TRANSFER AREA

Approximate the relationship between the heat transfer area to volume ratio and the vessel radius, assuming the vessel is externally jacketed and cylindrical.
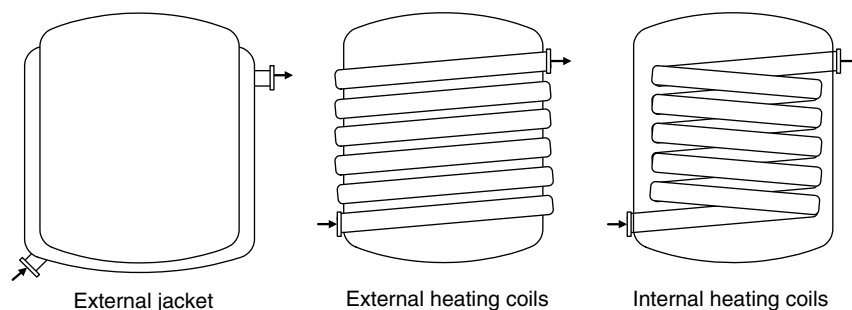

FIGURE 13.25   Schematics of common vessel heating arrangements.

Solution

The surface area of a cylinder is described by equation 13.24, neglecting the bottom surface:

$$SA = 2\pi rh \tag{13.24}$$

The volume of a cylinder can be defined by equation 13.25:

$$V = \pi r^2 h \tag{13.25}$$

As a result, the surface area to volume ratio for a cylinder is described by equation 13.26:

$$\frac{SA}{V} = \frac{2\pi rh}{\pi r^2 h} \propto \frac{1}{r} \tag{13.26}$$

Generally, the surface area to volume ratio for vessels is proportional to the inverse of the vessel radius.

The obvious impact of an increase in scale is a slower rate for heating or cooling steps relative to small vessels, assuming similar overall heat transfer coefficients and $(T_j - T_r)$ values. This must be taken into account when designing crystallizations in the laboratory, so that unrealistic heating or cooling rates are not specified. For any specified cooling rate, the temperature difference (ΔT) between the vessel jacket and its contents $(T_j - T_r)$ will increase with vessel size to match the heating or cooling times specified in the small-scale design. One effect of this larger $T_j - T_r$ is that during cooling, the wall temperature can be much lower than experienced in the laboratory equipment, potentially leading to nucleation near the wall at lower bulk temperatures than expected. Conversely, during heating the wall can be much hotter at large scale than small scale. Solids attached to vessel walls will often be exposed to higher temperatures as a result, possibly affecting purity.

EXAMPLE 13.7 SOLUTION COOLING

What is the temperature difference between the solution and jacket necessary to achieve a cooling rate of 1 K/min for the following vessels? The solution is ethanol (MW = 46 g/mol; $\rho = 0.79$ g/mL; $C_p = 112$ J/mol K), the jackets each have an overall heat transfer coefficient $U = 200$ W/m^2 K, with no limitations from the jacket services.

(a) 1 L lab reactor: $V_{\text{solvent}} = 0.8$ L; $A_{\text{vessel}} = 0.038$ m^2
(b) 300 gal pilot plant reactor: $V_{\text{solvent}} = 900$ L; $A_{\text{vessel}} = 4.0$ m^2
(c) 3000 gal plant reactor: $V_{\text{solvent}} = 9000$ L; $A_{\text{vessel}} = 19$ m^2

Solution

For the solution, the required heat flow is

$$\dot{Q} = m_{\text{solvent}} \cdot C_p \cdot \frac{\Delta T}{\Delta t} \tag{13.27}$$

For the heat flow between the jacket and solution:

$$\dot{Q} = U \cdot A_{\text{vessel}} \cdot (T_j - T_r) \tag{13.28}$$

Therefore, the temperature difference is

$$(T_j - T_r) = \frac{m_{\text{solvent}} \cdot C_p}{U \cdot A_{\text{vessel}}} \cdot \frac{\Delta T}{\Delta t} \tag{13.29}$$

And the temperature differences required are

(a) $(T_j - T_r) = \dfrac{m_{\text{solvent}} \cdot C_p}{U \cdot A_{\text{vessel}}} \cdot \dfrac{\Delta T}{\Delta t}$

$$= \frac{(0.8\,\text{L} \cdot 790\,\text{g/L}) \cdot (112\,\text{J/mol K} \cdot 1\,\text{mol}/46\,\text{g})}{200\,\text{J/s m}^2\,\text{K} \cdot 0.038\,\text{m}^2}$$

$$\cdot \frac{1\,\text{K}}{60\,\text{s}} = 3.4\,\text{K}$$

(b) $(T_j - T_r) = \dfrac{(900\,\text{L} \cdot 790\,\text{g/L}) \cdot (112\,\text{J/mol K} \cdot 1\,\text{mol}/46\,\text{g})}{200\,\text{J/s m}^2\,\text{K} \cdot 4.0\,\text{m}^2}$

$$\cdot \frac{1\,\text{K}}{60\,\text{s}} = 36\,\text{K}$$

(c) $(T_j - T_r) = \dfrac{(9000\,\text{L} \cdot 790\,\text{g/L}) \cdot (112\,\text{J/mol K} \cdot 1\,\text{mol}/46\,\text{g})}{200\,\text{J/s m}^2\,\text{K} \cdot 19\,\text{m}^2}$

$$\cdot \frac{1\,\text{K}}{60\,\text{s}} = 76\,\text{K}$$

What is the relationship between the temperature difference and the vessel radius, assuming it is cylindrical, externally jacketed, and neglecting the bottom surface? Building on the relationship shown in equation 13.26, it can be shown that the temperature difference between the jacket and solution is proportional to the vessel radius for a given heating or cooling rate, equation 13.30.

$$(T_j - T_r) \propto \frac{V}{A_{\text{vessel}}} \cdot \frac{\Delta T}{\Delta t} \propto r \cdot \frac{\Delta T}{\Delta t} \tag{13.30}$$

Evaluating the jacket temperature may indicate potential issues for the scale-up of a process, but it is a conservative measure. A system can be evaluated in more detail by calculating the wall temperature, which the solution is actually in contact with. The wall temperature can be calculated from the overall heat transfer rate in equation 13.28 by equating it to the heat transfer rate across the liquid film between the wall and the bulk liquid:

$$U \cdot A_{\text{vessel}} \cdot (T_j - T_r) = h_i \cdot A_{\text{vessel}} \cdot (T_w - T_r) \tag{13.31}$$

In equation 13.31 above, h_i is the heat transfer coefficient for liquid film, which is typically of the form shown in equation 13.32 for Newtonian liquids:

$$h_i = a \cdot \left(\frac{k}{T}\right)\left(\frac{C_p\mu}{k}\right)^{\frac{1}{3}}\left(\frac{D^2N\rho}{\mu}\right)^b\left(\frac{\mu}{\mu_w}\right)^m \quad (13.32)$$

For equation 13.32, a, b, and m are empirical constants dependant on the mixing geometry, k is the thermal conductivity of the liquid, T is the tank diameter, C_p is the specific heat capacity of the liquid, μ is the liquid viscosity, D is the impeller diameter, N is the agitation rate, and ρ is the density of the liquid. All of the liquid physical properties are evaluated at the temperature of the bulk liquid, T_r, except μ_w which is evaluated at the wall temperature, T_w [32]. Since h_i is dependent on the wall temperature, it is common to iteratively solve for T_w, from an initial guess, until the calculated value from equation 13.31 equals the guess used for μ_w in equation 13.32.

Temperature control at larger scale involves a dynamic feedback loop to control the jacket services, often across several vessels. If tuning of the controller is inadequate, a temperature cycling of a couple degrees above and below a "constant" temperature set point can be observed. The mixing in the vessel may also lead to considerable temperature gradients through the vessel contents. These temperature fluctuations could promote ripening effects, which would not have been experienced on small scale.

Another primary issue associated with temperature is the thermal effect caused by added antisolvent or reactants, and the heat of crystallization. The effect of these energy terms is illustrated in equation 13.33 for a crystal growth only system with ideal mixing. For antisolvent additions, the dosing regimen (rate, temperature of addition) is designed into the crystallization often to minimize the $(T_{antisolvent} - T_r)$ term. Equation 13.33 can be used in conjunction with crystal growth kinetic equations to allow a more detailed process model to be constructed, and can be modified to incorporate additional energy balance terms (e.g., heat of reaction, heat of mixing, heat from nucleation processes) for reactive crystallizations and nucleation dominated crystallizations. In equation 13.33, m_r is the mass of reactor contents, ΔH_c is the enthalpy of crystallization, and $\dot{m}_{antisolvent}$ is the mass addition rate of antisolvent.

$$\frac{d\{m_rC_pT_r\}}{dt} = U \cdot A_{vessel}(T_j - T_r) + \Delta H_c k_{GM} A_c \sigma_1^g$$
$$+ C_{p,antisolvent}\dot{m}_{antisolvent}(T_{antisolvent} - T_r)$$
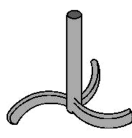$$(13.33)$$

13.6.2 Mixing Considerations

While the heat transfer considerations for crystallization scale-up are straightforward, those for mixing are increasingly complex, due to the wide variety of possible vessel configurations. Common impeller types include pitched-blade turbine, flat-blade turbine, curved-blade turbine, disc turbine, hydrofoil, retreat curve, propeller, and anchor, which are illustrated in Figure 13.26.

Mixing scale-up can be considered in three primary ways—geometrically, where the vessel and agitation configuration maintain the same shape and relative sizes, kinematically, where the relative velocities are maintained, and dynamically, where the relative forces are maintained [31]. The appropriate scale-up approach is dependent on the specific crystallization. The most common considerations for mixing scale-up for crystallization processes are provided in Table 13.7, including useful relationships for comparing geometric, kinematic, and dynamic similarities.

Vessel geometry (Figure 13.27) is a significant factor in mixing, but even when maintaining geometric similarity, on scale-up it is not possible to achieve both kinematic and dynamic similarity simultaneously, demonstrated illustratively in Figure 13.28.

Kinematic similarity is commonly compared using impeller tip speed or specific flow, but impeller, wall, or average

Pitched-blade turbine	Flat-blade turbine	Curved-blade turbine	Disc turbine
Po = 1.3 Fl = 0.8	Po = 2.0 Fl =1.0	Po = 2.0 Fl = 1.0	Po = 5.0 Fl = 0.7
Hydrofoil	Propeller	Retreat curve	Anchor
Po = 0.3 Fl = 0.6	Po = 0.8 Fl = 0.5	Po = 0.4 Fl = 0.3	Po = 0.6 Fl = 0.5

Copyright Chemineer 2010. Reprinted with permission of Chemineer, Inc.
Copyright Pfaudler 2010. Reprinted with permission of Pfaudler, Inc.

FIGURE 13.26 Common impeller types with typical power and flow numbers [17, 33–36].

TABLE 13.7   Useful Mixing Calculations [17, 33, 36]

| Parameter	Formula	Description
Scale ratio (−)	$s = \dfrac{D_1}{D_2} = \dfrac{T_1}{T_2} = \cdots$	Ratio of geometric dimensions between two vessels (Figure 13.27)
Reynold's number (−)	$\text{Re} = \dfrac{\rho N D^2}{\mu}$	Ratio of inertial to viscous forces and describes flow regime: Laminar—$Re < {\sim}10$ and $Po \propto Re^{-1}$ Transitional—$10 < Re < 10^4$ Turbulent—$Re > 10^4$; Po and $Fl = $ constant
Power number (−)	$Po = \dfrac{P}{\rho N^3 D^5}$	Characteristic impeller drag coefficient
Flow number (−)	$Fl = \dfrac{Q}{ND^3}$	Characteristic impeller discharge flow rate
Specific flow (1/s)	$\dfrac{Q}{V} = \dfrac{Fl N D^3}{V}$	Impeller discharge flow rate normalized by the fluid volume
Tip speed (m/s)	$v_T = \pi D N$	Impeller tip speed
Energy dissipation rate (W/m^3)	$\dfrac{P}{V} = \dfrac{Po \rho N^3 D^5}{V}$	Power dissipated by the impeller normalized by the fluid volume
Just suspension speed (rps)	$N_{js} = s\left(\dfrac{\mu}{\rho_l}\right)^{0.1}\left(\dfrac{g \cdot \Delta\rho}{\rho_l}\right)^{0.45} X^{0.13} d_p^{\,0.2} D^{-0.85}$	Minimum speed for complete suspension [37]
Mixing time (s)	$\theta_{\text{turbulent}} = C_1 \dfrac{T^{1.5} H^{0.5}}{Po^{1/3} N D^2}$ $\theta_{\text{transitional}} = C_2 \dfrac{T^{1.5} H^{0.5}}{Po^{2/3} Re N D^2}$	Time to achieve 95% homogeneity

D is the impeller diameter (m); T is the tank diameter (m); N is the impeller speed (1/s); ρ is the density (kg/m^3); μ is the viscosity (kg/m s); V is the fluid volume (m^3); s is the geometric constant; $\Delta\rho$ is the solid–liquid density difference (kg/m^3); X is the mass fraction solids (%); g is the gravitational acceleration (m^2/s); d_p is the particle diameter (m); H is the tank fill height (m); and C_1 and C_2 are the empirical constants (−); P is the impeller power (J/s).

shear rates can also be used. These can affect secondary nucleation during a crystallization process by causing crystal breakage, or attrition, through the crystal–impeller and crystal–wall impacts. Another kinematic consideration is solids suspension, typically evaluated with the just suspended agitation rate, or with cloud height prediction. Insufficient agitation could lead to stratification of the crystals, which could have the effect of growth dispersion by different crystal sizes residing in different mixing regimes of the vessel. Operationally, settling of product could cause issues transferring the slurry out of the vessel by blocking the bottom valve.

Dynamic similarity is commonly compared using energy dissipation rate, or the amount of energy transferred from the impeller to the fluid. The energy dissipation rate can affect the growth rate of crystals by changing the size of the diffuse boundary layer and, correspondingly, the mass transfer rate of bulk solute to the crystal surface. A lack of dynamic similarity could be manifested through a change in the crystal habit or aspect ratios, manipulating the independent crystal face growth rates. Additionally, secondary nucleation may be promoted if the energy dissipation rate is not sufficient to maintain the crystal growth rate, causing the system to maintain or increase its level of supersaturation. Depending on the mode of crystallization, another dynamic consideration for scale-up could be the mixing times, or degree of solution homogeneity. Crystallizations employing the addition of an antisolvent could be sensitive to the localized concentrations of the solvents since the solvent composition impacts the solubility and supersaturation. By extension, this principle can also apply to a reagent addition for a reactive crystallization. It should be noted that in these instances the addition point and geometry of the addition nozzle will have a significant impact on the mixing time.

This section covered conventional batch equipment and the most common considerations. However, specialized equipment and techniques can be utilized for modified crystallization mixing (e.g., to manipulate nucleation or attrition), including impinging jets, fluidized beds, sonication, and homogenizers [3].
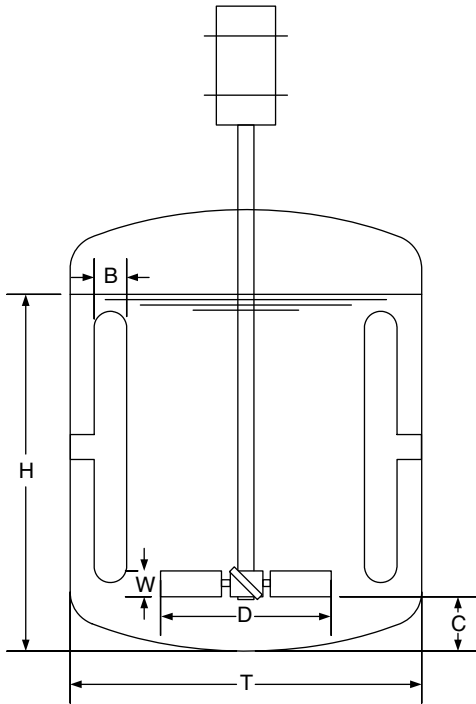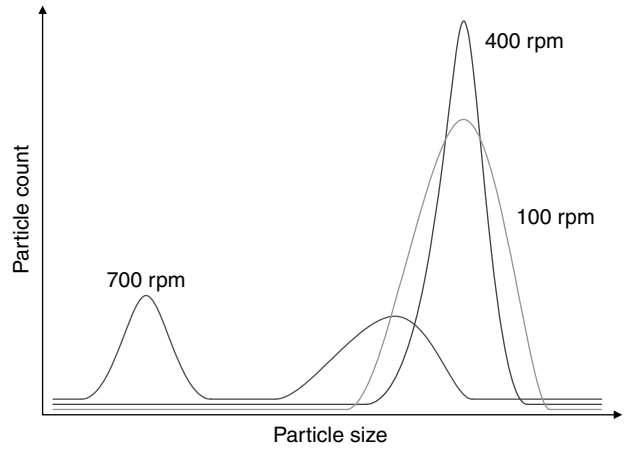
FIGURE 13.27 Illustration of geometric dimensions for an agitated vessel.

EXAMPLE 13.8   CRYSTALLIZATION MIXING

Given the product particle size distributions for a crystallization process evaluated at lab scale in Figure 13.29, what is the optimal agitation speed? And what are the likely explanations for the other two size distributions?

Solution
The narrowest particle size distribution was observed at 400 rpm, making that the most desirable of the three agitation rates. The lower agitation rate, 100 rpm, did not have suffi-

FIGURE 13.28 Power per unit volume scale-up comparison for constant: $A = Q/V$, $B = \theta_{\text{turbulent}}$, $C = P/V$, $D = N_{\text{js}}$, $E = v_{\text{T}}$, $F = Re$.

FIGURE 13.29 Lab-scale particle size distribution results. See Example 13.8 for additional details.

cient suspension of the particles, leading to stratification and growth dispersion, evidenced by a broader distribution. The higher agitation rate, 700 rpm, led to attrition and breakage of the particles, evidenced by a bimodal distribution.

The lab impeller used to generate these results was 70 mm in diameter and the process is to be scaled to a plant vessel with a 700 mm diameter impeller. Assuming geometric similarity between the vessels and impellers, what agitation rate would be required to maintain the optimum conditions by

$$s = \frac{H_{\text{lab}}}{H_{\text{plant}}} = \frac{T_{\text{lab}}}{T_{\text{plant}}} = \frac{D_{\text{lab}}}{D_{\text{plant}}} = \frac{70 \text{ mm}}{700 \text{ mm}} = 0.1$$

$$V \approx \frac{\pi}{4} T^2 H \Rightarrow \frac{V_{\text{lab}}}{V_{\text{plant}}} \approx s^3$$

(a) maintaining constant energy dissipation rate?

$$\left(\frac{P}{V}\right)_{\text{lab}} = \left(\frac{P}{V}\right)_{\text{plant}}$$

$$\frac{Po\rho N_{\text{lab}}^3 D_{\text{lab}}^5}{V_{\text{lab}}} = \frac{Po\rho N_{\text{plant}}^3 D_{\text{plant}}^5}{V_{\text{plant}}}$$

$$N_{\text{plant}}^3 = N_{\text{lab}}^3 \cdot \frac{D_{\text{lab}}^5}{D_{\text{plant}}^5} \cdot \frac{V_{\text{plant}}}{V_{\text{lab}}}$$

$$N_{\text{plant}} = N_{\text{lab}} \cdot \left(s^5 \frac{1}{s^3}\right)^{1/3}$$

$$N_{\text{plant}} = N_{\text{lab}} \cdot s^{2/3} = 200 \cdot 0.1^{2/3} = 86 \text{ rpm}$$

(b) maintaining constant specific flow?

$$\left(\frac{Q}{V}\right)_{\text{lab}} = \left(\frac{Q}{V}\right)_{\text{plant}}$$

$$\frac{FlN_{\text{lab}}D_{\text{lab}}^3}{V_{\text{lab}}} = \frac{FlN_{\text{plant}}D_{\text{plant}}^3}{V_{\text{plant}}}$$

$$N_{\text{plant}} = N_{\text{lab}} \cdot \frac{D_{\text{lab}}^3}{D_{\text{plant}}^3} \cdot \frac{V_{\text{plant}}}{V_{\text{lab}}}$$

$$N_{\text{plant}} = N_{\text{lab}} \cdot s^3 \cdot \frac{1}{s^3}$$

$$N_{\text{plant}} = N_{\text{lab}} = 400 \text{ rpm}$$

(c) maintaining constant tip speed?

$$v_{T\text{lab}} = v_{T\text{plant}}$$

$$\pi D_{\text{lab}} N_{\text{lab}} = \pi D_{\text{plant}} N_{\text{plant}}$$

$$N_{\text{plant}} = N_{\text{lab}} \cdot \frac{D_{\text{lab}}}{D_{\text{plant}}}$$

$$N_{\text{plant}} = N_{\text{lab}} \cdot s = 400 \cdot 0.1 = 40 \text{ rpm}$$

(d) maintaining constant blend time?

$$\text{Re} = \frac{\rho N D^2}{\mu} > 10^4 \text{ for turbulent regime} \Rightarrow \frac{\rho}{\mu} > \frac{10^4}{ND^2}$$

$$\frac{\rho}{\mu} > 3 \times 10^5 \text{ for lab impeller}$$

$$\frac{\rho}{\mu} > 1 \times 10^5 \text{ for plant impeller assuming}$$

minimum rate of 10 rpm

$$\frac{\rho}{\mu} \approx \frac{1000}{0.001} = 1 \times 10^6 \text{ for common solvents,}$$

therefore the turbulent regime can be assumed

$$\theta_{\text{turbulent lab}} = \theta_{\text{turbulent plant}}$$

$$C_1 \frac{T_{\text{lab}}^{3/2} H_{\text{lab}}^{1/2}}{Po^{1/3} N_{\text{lab}} D_{\text{lab}}^2} = C_1 \frac{T_{\text{plant}}^{3/2} H_{\text{plant}}^{1/2}}{Po^{1/3} N_{\text{plant}} D_{\text{plant}}^2}$$

$$N_{\text{plant}} = N_{\text{lab}} \cdot \left(\frac{T_{\text{plant}}}{T_{\text{lab}}}\right)^{3/2} \cdot \left(\frac{H_{\text{plant}}}{H_{\text{lab}}}\right)^{1/2} \cdot \left(\frac{D_{\text{lab}}}{D_{\text{plant}}}\right)^2$$

$$N_{\text{plant}} = N_{\text{lab}} \cdot \left(\frac{1}{s}\right)^{3/2} \cdot \left(\frac{1}{s}\right)^{1/2} \cdot s^2$$

$$N_{\text{plant}} = N_{\text{lab}} = 400 \text{ rpm}$$

(e) maintaining solids suspension?

$$\frac{N_{\text{js plant}}}{N_{\text{js lab}}} = \frac{D_{\text{plant}}^{-0.85}}{D_{\text{lab}}^{-0.85}}$$

$$N_{\text{js plant}} = N_{\text{js lab}} \cdot \left(\frac{1}{s}\right)^{-0.85}$$

$$= N_{\text{js lab}} \cdot s^{0.85} = 400 \cdot 0.1^{0.85} = 57 \text{ rpm}$$

What agitation rate should be utilized in the plant to scale-up this crystallization? Even for this simplified example, selecting just the agitation rate for scale-up is not straightforward. Based on the limited information provided, the goal is to scale-up the process and maintain suspension of the particles with sufficient mixing, yet avoid attrition by excessive mixing. To maintain the solids suspension an agitation rate of at least 57 rpm would be appropriate. However, this rate does not ensure homogeneity in the solution as it applies only to a just suspended criteria. To improve mixture homogeneity while minimizing the chance for attrition, scaling up while maintaining constant energy dissipation rate (86 rpm on scale) is a reasonable first choice. After experience on scale, the approach would be revisited to confirm suitability.

13.6.3 Damköhler Numbers

A useful approach for evaluating crystallization scale-up and mixing sensitivity is the use of Damköhler numbers, Da[3]. The Damköhler number is a dimensionless group traditionally used to compare reaction timescales to other phenomena, such as mass transport or residence time. Depending on the mode of crystallization, applicable Damköhler numbers may include

$$Da_{\text{nucleation}} = \frac{\text{mixing time}}{\text{induction time}}$$

$$Da_{\text{growth}} = \frac{\text{mixing time}}{\text{crystal growth time}}$$

$$Da_{\text{reaction}} = \frac{\text{mixing time}}{\text{reaction time}}$$

In general, low Da values suggest that mixing will have a minimal effect, while increasing Da values suggesting increasing criticality of the mixing. For example, at low value of Da_{growth} mixing would have a minimal effect on the resulting particle size distribution. However, at high values, slow mixing and fast nucleation or crystal growth, mixing would impact the particle size distribution since localized concentrations would lead to variable nuclei generation or crystal growth rates throughout the solution. The value of a Damköhler number will depend on the specific definition used; generally though, an order of magnitude constitutes a low or high Da value (i.e., <0.1 and >10, respectively).

For reactive crystallization processes, $Da_{reaction}$ has to be considered along with $Da_{nucleation}$ or Da_{growth} when analyzing the mixing criticality. For example, at high $Da_{reaction}$ values, fast reaction relative to mixing, high-localized concentrations of product could be generated. Combined with a high $Da_{nucleation}$ or Da_{growth}, the fast nucleation or growth rates would make mixing critical to the product. However, if combined with a low $Da_{nucleation}$ or Da_{growth}, product generated by the reaction may be distributed evenly throughout the vessel before affecting nucleation or crystal growth. Alternatively, at low $Da_{reaction}$ values, the reactants may be evenly distributed throughout the vessel before reaction, leading to a uniform product concentration and the mixing sensitivity solely due to the nucleation or growth.

The discussion above provides the concepts for utilizing Damköhler numbers to evaluate crystallizations, but the application does not have to be limited to these approaches. For example, one could also compare reaction rate and crystal growth rate directly for another Damköhler number applicable to reactive crystallizations.

13.6.4 Cooling Crystallization Considerations

Cooling crystallizations are commonly employed processes and the most typical considerations for their scale-up are as follows:

- Maintaining a cooling profile
- Managing the wall temperature
- Mixing that can impact both heat and mass transfer

As illustrated in the example regarding cooling a solution, scaling up a cooling profile for a batch process in typical equipment requires considerably larger temperature differentials when compared to lab scale. At scale, the wall temperature will be somewhat cooler than the bulk solution. Prior to seeding, the lower wall temperature could then lead to undesired nucleation by generating a higher localized supersaturation near the wall, which may exceed the metastable limit and induce nucleation. Alternatively, if the wall temperature is managed by controlling the solution–jacket temperature differential, the time required to cool would potentially be extended beyond the nucleation induction time, again leading to undesired nucleation. Often at scale there will be a limit beyond which the cooling rate cannot be maintained, a threshold rate. Design approaches must take into consideration the heat transfer characteristics of the manufacturing vessel so that practical cooling rates and timescales are incorporated into crystallization design. As no reagent additions or reactions are occurring, mixing considerations typically involve the assurance of adequate suspension without significant breakage; scaling by constant energy dissipation rate is often a good starting point for mixing calculations.

13.6.5 Antisolvent Crystallization Considerations

The most typical scale-up considerations for antisolvent crystallizations are as follows:

- Maintaining an antisolvent addition rate profile
- Managing temperature gradients due to the antisolvent addition
- Mixing that can impact both heat and mass transfer

Antisolvent crystallizations can be complicated by differences in temperature between the antisolvent and the solvent. If the antisolvent being added is at a different temperature than the crystallization solution, heat has to be added or removed to maintain the desired solution temperature (equation 13.33). Additionally, the equipment setup and mixing will significantly impact the distribution of the antisolvent and equilibration of heat. Therefore, antisolvent crystallizations have more potential to be sensitive to mixing than a common cooling crystallization. The simplest approach to minimize heat transfer or temperature considerations for an antisolvent addition is to adjust the antisolvent to the same temperature as the crystallization solution prior to addition. Addressing the distribution of antisolvent during an addition does not have a standard approach. Evaluating a Damköhler number provides a starting point, especially for comparing demonstrated laboratory conditions to proposed conditions at scale. Since mixing times generally increase with scale, it may be necessary to increase the antisolvent addition time accordingly to minimize impacts to the crystallization from localized concentrations. Effective mixing at the point of antisolvent introduction is especially critical to reduce the probability of nucleation due to the high local antisolvent concentration at that point. These effects are often investigated as sensitivity studies on small scale (i.e., $<20\,L$) by varying the addition geometry and rate and examining their sensitivity to particle size. For situations in which Da is small and a growth mechanism is employed, scaling up mixing by constant energy dissipation rate is a reasonable starting point, with increases in agitation rate toward a constant mixing time with increasing Da.

13.6.6 Reactive Crystallization Considerations

Reactive crystallizations can be more complex than the other modes of crystallization due to the addition of the reaction rate to the already present rates of mixing, mass transfer, and crystal growth. The most typical considerations for their scale-up are as follows:

- Maintaining a reagent addition rate profile
- Managing temperature gradients due to the reagent addition and heat of reaction
- Mixing that can impact both heat and mass transfer

Assuming the reaction requires the addition of a reagent, the heat transfer considerations for reactive crystallizations are similar to those of antisolvent crystallizations. However, it is more likely that the heat of reaction, and even the heat of addition in the case of acids or bases, will be significant and require significant jacket compensation for heat removal. Again, Damköhler numbers would provide a useful evaluation of a process and its scale-up. For reactive crystallizations the rate processes include the reagent addition, reaction, mixing, and nucleation, and/or growth. A thorough assessment requires the comparison of all of these components of the process. By comparing the reagent addition rate and the reaction rate it may be determined whether the reaction is addition rate controlled, where the reactant is consumed as fast as it is added, or if there is accumulation of the reagent. In the first case, it would be the addition rate that needs to be compared to the mixing times and nucleation and growth rates, but in the second it would be the reaction rate. This also highlights a potential method of adjusting a process for improved control—selecting a reagent addition rate slow enough to prevent reagent accumulation. Because of the number of simultaneous rate processes, reactive crystallizations tend to be the most problematic to scale-up.

13.6.7   Evaporative Crystallizations Considerations

The most typical scale-up considerations for evaporative crystallizations are as follows:

- Maintaining an evaporation rate profile
- Managing the wall temperature and encrustation
- Mixing that can impact both heat and mass transfer

Evaporative crystallizations encounter heat transfer limitations during scale-up that are similar to cooling crystallizations. With the reduced heat transfer area to volume on scale, larger temperature differences between the jacket and solution are required to maintain a desired evaporation rate. During scale-up, it is common to utilize higher jacket temperatures, since the solution temperature is fixed at the boiling point. Additional considerations due to the increased jacket temperature include chemical degradation, encrustation, nucleation, and foaming, each discussed briefly in this section. Chemical degradation of the product may be encountered with the higher localized temperatures at the vessel walls. The higher localized temperatures at the wall also promote faster evaporation of the solvent there, which combined with the reducing solution volume can lead to a buildup of product crystals on the wall above the solution surface. This encrustation may also exhibit increased levels of degradation since the solids are exposed to the heat from the jacket for the remainder of the process. If a process is initially designed as an evaporative crystallization at atmospheric pressure, reduction of the operating pressure can be the easiest approach to address the need for higher jacket temperatures. Reduced pressure alone will not address encrustation above the liquid level, and it increases the potential for foaming, which is commonly exacerbated by the presence of small particles. As a consequence of each of these potential issues, a reduced evaporation rate (using low $T_j - T_r$ values) and seeding at relatively high proportions may be required to successfully scale-up this mode of crystallization. Similar to cooling crystallizations, scaling by constant energy dissipation rate is a reasonable starting point for design.

REFERENCES

1. Mullin JW. *Crystallization*, 4th edition, Elsevier Butterworth-Heinemann, 2001.
2. Myerson AS. *Handbook of Industrial Crystallization*, 2nd edition, Butterworth-Heinemann, 2002.
3. Tung H, et al. *Crystallizations of Organic Compounds: An Industrial Perspective*, Wiley, Hoboken, 2009.
4. Sisko J, Oh LM, et al. Process development of a novel pleuromutilin-derived antibiotic. *Org. Process Res. Dev.* 2009; 13: 729–738.
5. Henck JO, Kuhnert-Brandstatter M. Demonstration of the terms enantiotropy and monotropy in polymorphism research exemplified by flurbiprofen. *J. Pharmaceut. Sci.* 1999; 88 (1): 103–108.
6. Byrn S, et al. Pharmaceutical solids: a strategic approach to regulatory considerations. *Pharmaceut. Res.* 1995; 12 (7): 945–954.
7. Henck J, Kuhnert-Brandstatter M. *J. Pharmaceut. Sci.* 1999; 88 (1): 103–108.
8. Vogt FG, et al. Physical, crystallographic, and spectroscopic characterization of a crystalline pharmaceutical hydrate: understanding the role of water. *Crystal Growth Design* 2006; 6 (10): 2333–2354.
9. Zaworotko MJ, et al. Crystal engineering of the composition of pharmaceutical phases: multiple-component crystalline solids involving carbamazepine. *Crystal Growth Design* 2003; 13 (6): 909–919.
10. Childs SL, et al. Crystal engineering approach to forming cocrystals of amine hydrochlorides with organic acids, molecular complexes of fluoxetine, hydrochloride with benzoic, succini, and fumaric acids. *J. Am. Chem. Soc.* 2004; 126 (41): 13335–13342.
11. Bernstein J. *Polymorphism in Molecular Crystals*, 1st edition, Oxford University Press, 2002.
12. Hilfiker R. *Polymorphism in the Pharmaceutical Industry*, 1st edition, Wiley-VCH, 2006.
13. Gibson M. *Pharmaceutical Preformulation and Formulation*, 1st edition, Interpharm/CRC, 2004.

14. Chemburkar SR, et al. Dealing with the impact of ritonavir polymorphs on the late stages of bulk. *Org. Process Res. Dev.* 2000; 4: 413–417.

15. Liu R. *Water-Insoluble Drug Formulation*, Interpharm Press, 2000.

16. Santomaso A, Lazzaro P, Canu P. Powder flowability and density ratios: the impact of granules packing. *Chem. Eng. Sci.* 2003; 58 (13): 2857–2874.

17. Perry RH, Green DW, Maloney JO. *Perry's Chemical Engineers' Handbook*, 7th edition, McGraw-Hill, 1997.

18. Togkalidou T, et al. Experimental design and inferential modeling in pharmaceutical crystallization. *AIChE J.* 2001; 47 (1): 160–168.

19. Zhu H, Yuen C, Grant DJW. Influence of water activity in organic solvent + water mixtures on the nature of the crystallizing drug phase 1-theophylline. *Int. J. Pharmaceut.* 1996; 135: 151–160.

20. Matthews HB, Rawlings JB. Batch crystallization of a photochemical: modeling, control, and filtration. *AIChE J.* 1998; 44 (5): 1119–1127.

21. Larson M, Khambaty S. Crystal regeneration and growth of small crystals in contact nucleation. *Ind. Eng. Chem. Fundam.* 1978; 17 (3): 160–165.

22. Kashchiev D. *Nucleation: Basic Theory with Applications*, 1st edition, Butterworth-Heinemann, 2000.

23. Dell'Orco P, Patience D, Rawlings J. Optimal operation of a seeded pharmaceutical crystallization with growth-dependent dispersion. *Org. Process Res. Dev.* 2004; 8 (4): 609–615.

24. Kougoulos E, et al. Use of focused beam reflectance measurement (FBRM) and process video imaging (PVI) in a modified mixed suspension mixed product removal (MSMPR) cooling crystallizer. *J. Crystal Growth* 2005; 273 (3–4): 529–534.

25. Nocent M, et al. Definition of a solvent system for spherical crystallization of salbutamol sulfate by quasi-emulsion solvent diffusion (QESD) method. *J. Pharmaceut. Sci.* 2001; 90 (10): 1620–1627.

26. Bratz. [Online] http://brahms.scs.uiuc.edu.

27. Rawlings. [Online] http://jbrwww.che.wisc.edu.

28. Ramkrishna D. *Population Balances: Theory and Applications to Particulate Systems in Engineering*, 1st edition, Academic Press, 2000.

29. Cote A, Zhou G, Stanik M. A novel crystallization methodology to ensure isolation of the most stable crystal form. *Org. Process Res. Dev.* 2009; 13: 1276–1283.

30. McCabe WL, Smith JC, Harriot P. *Unit Operations of Chemical Engineering*, 6th edition McGraw-Hill, 2001.

31. Schmidt B, et al. Application of process modelling tools in the scale-up of pharmaceutical. *Org. Process Res. Dev.* 2004; 8: 998–1008.

32. Geankoplis CJ. *Transport Processes and Unit Operations*, 3rd edition, Prentice Hall, 1993.

33. McConville FX. *The Pilot Plant Real Book: A Unique Handbook for the Chemical Process Industry*, 2nd edition, Fxm Engineering & Design, 2006.

34. Chemineer Impellers. [Online] http://www.chemineer.com/impellers.php.

35. Pfaudler Impellers. [Online] http://www.pfaudler.com/mixing_systems.php.

36. Kirk RE, et al. *Encylopedia of Chemical Technology*, 4th edition, Wiley, 1998.

37. Zwietering TN. Suspending of solid particles in liquids by agitators. *Chem. Eng. Sci.* 1958; 8: 244–253.